Reducing FASN expression sensitizes acute myeloid leukemia cells to differentiation therapy

Magali Humbert[1,2,#], Kristina Seiler[1,3], Severin Mosimann[1], Vreni Rentsch[1], Sharon L. McKenna[2,4], Mario P. Tschan[1,2,3]

[1]Institute of Pathology, Division of Experimental Pathology, University of Bern, Bern, Switzerland
[2]TRANSAUTOPHAGY: European network for multidisciplinary research and translation of autophagy knowledge, COST Action CA15138
[3]Graduate School for Cellular and Biomedical Sciences, University of Bern, Bern, Switzerland,
[4]Cancer Research, UCC, Western Gateway Building, University College Cork, Cork, Ireland.

[#]Corresponding Author: Magali Humbert, Institute of Pathology, Division of Experimental Pathology, University of Bern, Murtenstrasse 31, CH-3008 Bern, Switzerland, E-mail: magali.humbert@pathology.unibe.ch, Tel: +41 31 632 8744, Fax: +41 31 381 3412

Running Title: FASN impairs TFEB activity in AML

Key words: FASN/AML/ATRA/TFEB/mTOR/autophagy

Abstract

Fatty acid synthase (FASN) is the only human lipogenic enzyme available for *de novo* fatty acid synthesis and is often highly expressed in cancer cells. We found that FASN mRNA levels were significantly higher in acute myeloid leukemia (AML) patients than in healthy granulocytes or $CD34^+$ hematopoietic progenitors. Accordingly, FASN levels decreased during all-*trans* retinoic acid (ATRA)-mediated granulocytic differentiation of acute promyelocytic leukemia (APL) cells, partially via autophagic degradation. Furthermore, our data suggests that inhibition of FASN expression levels using RNAi or (-)-epigallocatechin-3-gallate (EGCG), accelerates the differentiation of APL cell lines and significantly re-sensitized ATRA refractory non-APL AML cells. FASN reduction promoted translocation of transcription factor EB (TFEB) to the nucleus, paralleled by activation of CLEAR network genes and lysosomal biogenesis. Lysosomal biogenesis was activated, consistent with TFEB transcriptional activation of CLEAR network genes.

Together, our data demonstrate that inhibition of FASN expression in combination with ATRA treatment facilitates granulocytic differentiation of APL cells and may extend differentiation therapy to non-APL AML cells.

Introduction

While traditional chemotherapy and radiotherapy target highly proliferative cancer cells, differentiation-inducing therapy aims to restore differentiation programs to drive cancer cells into maturation and ultimately into cell death. Differentiation therapies are associated with lower toxicity compared to classical cytotoxic therapies. The success of this therapeutic approach is exemplified by the introduction of all-*trans* retinoic acid (ATRA) in 1985 to treat acute promyelocytic leukemia (APL) (Wang & Chen, 2008). The introduction of ATRA into the treatment regimen changed APL from being one of the most aggressive acute myeloid leukemia (AML) subtypes with a fatal course often within weeks only, to a curable disease with a complete remission rate of up to 95% when combined with anthracycline-based chemotherapy or arsenic trioxide (Wang & Chen, 2008). APL is characterized by translocations involving the C-terminus of the retinoic acid receptor alpha (RARA) on chromosome 17 and genes encoding for aggregate prone proteins. Promyelocytic leukemia (PML)-RARA is the most frequently expressed fusion protein. It is encoded by the translocation t(15;17) and has a dominant negative effect on RARA. RARA transcriptionally regulates multiple biological processes with a key role in differentiation (Germain *et al*, 2006). Several reports suggest a beneficial effect of ATRA in combination therapies in non-APL AML cells (Su *et al*, 2015; Marchwicka *et al*, 2014; Schenk *et al*, 2012). Unfortunately, a variety of intrinsic resistance mechanisms in non-APL AML have been identified such as SCL overexpression, expression of PRAME and epigenetic silencing or mutation of RARA (Rice *et al*, 2004; Bullinger *et al*, 2013; Petrie *et al*, 2009; Altucci & Gronemeyer, 2001). Deciphering the mechanisms active during ATRA-mediated differentiation at the molecular level will support the translation of differentiation therapy to non-APL AML patients. We and others have demonstrated the importance of autophagy in ATRA induced granulocytic differentiation of APL

cells (Isakson *et al*, 2010; Wang *et al*, 2011; Jin *et al*, 2018; Humbert *et al*, 2017; Brigger *et al*, 2014b; Orfali *et al*, 2019). Autophagy is an intracellular degradation mechanism that ensures dynamic recycling of various cytoplasmic contents (Feng *et al*, 2014). We thus aim to understand the role of autophagy in granulocytic differentiation and to define key druggable autophagy targets in this process.

Endogenous synthesis of fatty acids is catalyzed by fatty acid synthase (FASN), the only human lipogenic enzyme able to perform *de novo* synthesis of fatty acids (Asturias *et al*, 2005; Maier *et al*, 2006). FASN is frequently overexpressed in a variety of tumor types including leukemias (Pizer *et al*, 1998; Visca *et al*, 2004; Bandyopadhyay *et al*, 2005; Alo *et al*, 1996; Shurbaji *et al*, 1996; Rashid *et al*, 1997; Diaz-Blanco *et al*, 2007) while its expression in healthy adult tissues is low (Weiss *et al*, 1986), with the exception of the cycling endometrium (Pizer *et al*, 1997) and lactating breast (Maningat *et al*, 2009). Interestingly, FASN is upregulated in tumor associated myeloid cells where it activates nuclear receptor peroxisome-proliferator-activated receptor beta/delta (PPARβ/δ) (Park *et al*, 2015), a key metabolic transcription factor in tumorigenesis (Peters & Gonzalez, 2009; Zuo *et al*, 2009). Of note, activation of PPARβ/δ regulates anti-inflammatory phenotypes of myeloid cells in other biological contexts such as atherosclerosis and obesity (Han Jung-Kyu *et al*, 2008; Kang *et al*, 2008; Lee *et al*, 2003; Odegaard *et al*, 2008). We previously reported that (-)-epigallocatechin-3-gallate (EGCG) improved ATRA induced differentiation of APL cells by increasing the expression of death associated protein kinase 2 (DAPK2). Furthermore, EGCG treatment reduce FASN expression levels in selected breast cancer cell lines (Yeh *et al*, 2003). The increased FASN expression in cancer including leukemias, its function in tumor-associated myeloid cells and its

link to the differentiation enhancer DAPK2 prompted us to analyze the regulation and function of FASN during myeloid leukemic differentiation.

In the present study, we demonstrate that FASN expression is significantly higher in AML blasts partially due to low autophagic activity in those cells. We show that inhibiting FASN protein expression, but not its enzymatic activity, promotes differentiation of non-APL AML cells. Lastly, we link FASN expression to mTOR activation and inhibition of the key lysosomal biogenesis transcription factor TFEB.

Material and Methods

2.1. Primary cells, cell lines and culture conditions

Fresh leukemic blast cells from untreated AML patients at diagnosis were obtained from the Inselspital Bern (Switzerland) were classified according to the French-American-British classification and cytogenetic analysis. All leukemia samples had blast counts of ~90% after separation of mononuclear cells using a Ficoll gradient (Lymphoprep; Axon Lab AG, Switzerland), as described previously (Tschan *et al*, 2003). Protocols and use of 67 human samples acquired in Bern were approved by the Cantonal Ethical Committee at the Inselspital. The isolation of primary neutrophils (purity 95%) was performed by separating blood cells from healthy donors using polymorphprep (Axon Lab AG, Switzerland). $CD34^+$ cells from cord blood or bone marrow were isolated as described (Tschan *et al*, 2003).

The human AML cell lines, HT93, OCI/AML2, MOLM-13 and NB4 were obtained from the Deutsche Sammlung von Mikroorganismen und Zellkulturen GmbH (DSMZ, Braunschweig, Germany). All cell lines were maintained in RPMI-1640 with 10% fetal calf serum (FCS), 50 U/mL penicillin and 50 µg/mL streptomycin in a 5% CO_2-95% air humidified atmosphere at 37°C. For differentiation experiments, AML cells were treated with 1µM all-*trans* retinoic acid (ATRA; Sigma-Aldrich, Switzerland). Successful granulocyte differentiation was evidenced by CD11b surface expression measured by FACS.

293T cells were maintained in DMEM (Sigma-Aldrich, St. Louis, MO, USA), supplemented with 5% FBS, 1% penicillin/streptomycin, and 1% Hepes (Sigma-Aldrich, Switzerland), and kept in a 7.5%CO_2-95% air humidified atmosphere at 37°C.

2.2 Antibodies

Antibodies used were anti-FASN (3180; Cell Signaling, Switzerland), anti-LC3B (WB: NB600-1384, Novus biological, Switzerland; IF: 3868; Cell Signaling, Switzerland) anti-LAMP1 (14-1079-80; Thermofisher, Switzerland), anti-p62 (HPA003196 ; Sigma-Aldrich, Switzerland), anti-TFEB (4240; Cell Signaling, Switzerland) anti-ULK1(4776; Cell Signaling, Switzerland), anti p-ULK1 (Ser757) (6888; Cell Signaling, Switzerland), anti-ATG13 (6940 ; Cell Signaling, Switzerland), anti-pATG13 (Ser318) (600-401-C49; Rockland, Switzerland), anti p-mTOR (Ser2448) (5536; Cell Signaling, Switzerland), p4E-BP1 (Thr37/46) (2855; Cell Signaling, Switzerland), anti-α-tubulin (3873; Cell Signaling, Switzerland), anti-cleaved PARP (9541; Cell Signaling, Switzerland), anti yH2AX (2577; Cell Signaling, Switzerland) and anti-CD11b-PE (R0841; Dako, Switzerland).

2.3 Cell lysate preparation and western blotting

Whole cell extracts were prepared using UREA lysis buffer and 30-60µg of total protein was loaded on a 7.5% or 12% denaturing polyacrylamide self-cast gel (Bio-Rad, Switzerland). Blots were incubated with the primary antibodies in TBS 0.05% Tween-20 / 5% milk overnight at 4°C and subsequently incubated with HRP coupled secondary goat anti-rabbit (7074; Cell Signaling, Switzerland) and goat anti-mouse antibody (7076; Cell Signaling, Switzerland) at 1:5-10,000 for 1 h at room temperature. Blots were imaged using Chemidoc (Bio-Rad, Switzerland) and ImageLab software.

2.4 Lentiviral vectors

pLKO.1-puro lentiviral vectors expressing shRNAs targeting *FASN* (sh*FASN*_1: NM_004104.x-1753s1c1 and sh*FASN*_2: NM_004104.x-3120s1c1) were purchased from Sigma-Aldrich. An mCherry-LC3B lentiviral vector was kindly provided by Dr. Maria S. Soengas (CNIO, Molecular Pathology Program, Madrid, Spain). All vectors

149 contain a puromycin antibiotic resistance gene for selection of transduced
150 mammalian cells. Lentivirus production and transduction were done as described
151 (Rizzi *et al*, 2007; Tschan *et al*, 2003). Transduced NB4 cell populations were
152 selected with 1.5 µg/ml puromycin for 4 days and knockdown efficiency was
153 assessed by western blot analysis.

154 *2.5 Immunofluorescence microscopy*

155 Cells were prepared as previously described (Brigger *et al*, 2014b). Briefly, cells were
156 fixed and permeabilized with ice-cold 100% methanol for 4 min (LC3B and LAMP1
157 staining) or 2% paraformaldehyde for 7 min followed by 5 minutes in PBS 0,1%
158 TRITON X-100 (TFEB and tubulin staining) and then washed with PBS. Cells were
159 incubated with primary antibody for 1 h at room temperature followed by washing
160 steps with PBS containing 0.1% Tween (PBS-T). Cells were incubated with the
161 secondary antibody (anti-rabbit, 111-605-003 (Alexa Fluor® 647) 111-096-045
162 (FITC); anti-mouse, (Cy3) 115-605-003 (Alexa Fluor® 647); Jackson
163 ImmunoResearch, West Grove, PA, USA) for 1 h at room temperature. Prior to
164 mounting in fluorescence mounting medium (S3032; Dako, Switzerland) cells were
165 washed three times with PBS-Tween. Images were acquired on an Olympus
166 FluoView-1000 confocal microscope (Olympus, Volketswil, Switzerland) at 63x
167 magnification.

168 2.6 Acridine Orange staining

169 Cells were washed 3 times with PBS and resuspended in RPMI 10% FBS containing
170 5ug/mL Acridine Orange (A3568, Invitrogen, Switzerland) to a concentration of 0.2 x
171 10^6 cells per mL. Cells were then incubated at 37°C for 20 min and washed 3 times
172 with PBS. Acridine Orange staining was measured by FACS analysis using a 488nm

laser with 530/30 (GREEN) and 695/40 (RED) filters on a FACS LSR-II (BD Biosciences, Switzerland). Data were analyzed with FlowJo software (Ashland, OR, USA). The software derived the RED/GREEN ratio and we compared the distribution of populations using the Overton cumulative histogram subtraction algorithm to provide the percentage of cells more positive than the control.

2.7 Nitroblue tetrazolium reduction test

Suspension cells (5 x 10^5) were resuspended in a 0.2% nitro blue tetrazolium (NBT) solution containing 40ng/ml PMA and incubated 15min at 37°C. Cells were then washed with PBS and subjected to cytospin. Counterstaining was done with 0.5% Safranin O for 5min (HT90432; Sigma Aldrich, Switzerland). The NBT-positive and negative cells were scored under a light microscope (EVOS XL Core, Thermofisher, Switzerland).

2.8 Trypan blue exclusion counting

Trypan blue exclusion cell counting was performed to assess cellular growth. 20µL of cell suspension was incubated with an equal volume of 0.4% (w/v) trypan blue solution (Sigma-Aldrich, Switzerland). Cells were counted using a dual-chamber hemocytometer and a light microscope (EVOS XL Core, Thermofisher, Switzerland).

2.9 Real-time quantitative RT-PCR (qPCR).

Total RNA was extracted using the RNeasy Mini Kit and the RNase-Free DNase Set according to the manufacturer's protocol (Sigma-Aldrich, Switzerland). Total RNA was reverse transcribed using all-in-one RT-PCR (BioTool, Switzerland). Taqman® Gene Expression Assays for *BECN1*, *GABARAP*, *STK4,* and *WDR45* were Hs00186838_m1, Hs00925899_g1, Hs00178979_m1 and Hs01079049_g1,

196 respectively. Specific primers and probes for *HMBS* have been already described
197 (Tschan *et al*, 2003). Data represent the mean ± s.d. of at least two independent
198 experiments.

199 *2.10 Statistical analysis*

200 Nonparametric Mann-Whitney-U tests were applied to compare the difference
201 between two groups and Spearman Coefficient Correlation using Prism software
202 (GraphPad Software, Inc., Jolla, CA, USA). P-values < 0.05 were considered
203 statistically significant. The error bar on graphs represents the SD of at least two
204 biological replicates performed in two technical replicates

3.1. Primary AML blast cells express significantly higher FASN levels compared to mature granulocytes

Cancer cells frequently express high levels of FASN compared to their healthy counterparts (Pizer *et al*, 1998; Visca *et al*, 2004; Bandyopadhyay *et al*, 2005; Alo *et al*, 1996; Shurbaji *et al*, 1996; Rashid *et al*, 1997; Diaz-Blanco *et al*, 2007). We examined *FASN* mRNA expression in an AML patient cohort. *FASN* mRNA levels in AML samples (n=68) were compared to the levels in granulocytes (n=5) and $CD34^+$ human hematopoietic progenitor cells (n=3) from healthy donors. We found that *FASN* expression was significantly higher in AML patients compared to healthy granulocytes ($p<0.05$) (Figure 1A). We obtained similar findings by analyzing *FASN* expression in AML patient data available from the Bloodspot gene expression profile data base (Bagger *et al*, 2016) (Figure 1B). In addition, hematopoietic stem cells from healthy donors express significantly lower *FASN* mRNA transcript levels than AML blasts (Figure 1B). Next, we asked if FASN expression was altered during granulocytic differentiation of APL cells. We analyzed FASN protein expression following ATRA-induced differentiation of two APL cell lines, NB4 and HT93. ATRA treatment resulted in markedly reduced FASN protein levels from day two onwards (Figure 1C). This further suggests that high FASN expression is linked to an immature blast-like phenotype and that ATRA-induced differentiation reduces FASN levels.

3.2. FASN protein is degraded via macroautophagy during ATRA-induced granulocytic differentiation

We and others have demonstrated that autophagy gene expression is repressed in AML samples compared to granulocytes from healthy donors and that autophagy activity is essential for successful ATRA-induced APL differentiation (Isakson *et al*,

2010; Wang *et al*, 2011; Jin *et al*, 2018; Humbert *et al*, 2017; Brigger *et al*, 2014b; Watson *et al*, 2015; Orfali *et al*, 2015, 2019). The decrease in FASN expression upon ATRA-induced differentiation cannot be explained solely by transcriptional regulation due to the long half-life of this protein (1-3 days)(Volpe & Vagelos, 1976; Weiss *et al*, 1986). Moreover, FASN can be present inside autophagosomes, for instance in yeast and in the breast cancer cell line MCF7 (Dengjel *et al*, 2012; Suzuki *et al*, 2014). Therefore, we hypothesized that ATRA-induced autophagy participates in the degradation of FASN during differentiation of APL cells. To examine whether autophagy is involved in FASN degradation, we treated NB4 cells for 24h with different concentrations of Bafilomycin A1 (BafA1), a specific inhibitor of vacuolar-type H^+-ATPase (Yamamoto *et al*, 1998; Poole & Ohkuma, 1981), alone or in combination with ATRA. FASN protein was found to accumulate in the presence of BafA1, together with autophagy markers p62 and LC3B-II (Figure 2A). To validate these findings, we utilized NB4 cells stably expressing mCherry-LC3B. Cells were treated with different concentrations of BafA1 with or without ATRA for 24h and FASN as well as LC3B localization was assessed. Endogenous FASN (cyan) showed co-localization with mCherry-LC3B (red) in BafA1 and ATRA treated cells (Figure 2B). In addition, we found colocalization with endogenous FASN (red) and p62 (green) in NB4 parental cells treated with both ATRA and BafA1 for 24h (Figure 2C). It is possible that p62 may help to sequester FASN to the autophagosome. In summary, these data suggest that FASN is a target for autophagic degradation during granulocytic differentiation of APL cells.

We have previously shown that EGCG improves the response to ATRA in AML cells by inducing DAPK2 expression, a key kinase in granulocytic differentiation (Britschgi *et al*, 2010). Furthermore, EGCG was reported to decrease FASN expression (Yeh *et al*, 2003) and this was reproducible in our APL cell line model (Supplementary Figure

1A-B). Using different EGCG doses and treatment time points, we confirmed that EGCG improves ATRA induced differentiation in NB4 cells, as evidenced by increased NBT positive cells and CD11b surface expression (Supplementary Figure 1C-E). Importantly, increased differentiation when combining ATRA with EGCG was paralleled by enhanced autophagic activity (Supplementary Figure 1F-G). Autophagy induction was determined by quantifying endogenous, lipidated LC3B-II by western blotting and a dual-tagged mCherry-GFP-LC3B expression construct as described previously (Humbert *et al*, 2017; Gump & Thorburn, 2014; Klionsky *et al*, 2016). Autophagic flux quantification upon EGCG treatment was performed in the presence or absence of BafA1 (Klionsky *et al*, 2016). We found no significant changes in cell death or proliferation measured by DAPI staining and trypan blue exclusion, respectively (Supplementary Figure 2H-I). Co-treating NB4 parental cells with EGCG and ATRA as well as blocking autophagy using BafA1 for 24h, resulted in a higher accumulation of FASN protein (Figure 2D and Supplementary Figure 1J). Interestingly, we saw an accumulation of a band at the molecular weight of FASN dimer (Figure 2D and Supplementary Figure1J). Together, our data demonstrate that FASN can be degraded via autophagy during APL cell differentiation and that co-treatment with EGCG further promotes FASN protein degradation.

3.4. Inhibiting FASN protein expression but not its catalytic function accelerates ATRA-induced granulocytic differentiation in APL cell lines

Next, we evaluated the impact of modulating FASN expression and activity on myeloid differentiation. Therefore, we genetically inhibited FASN expression using lentiviral vectors expressing two independent shRNAs targeting *FASN* in the NB4 APL cell line model. Knockdown efficiency was validated by western blotting (Figure 3A). We found that ATRA treatment significantly reduced the doubling time

(Supplementary Figure 2A-B) and lowered accumulation of DNA damage as indicated by yH2AX immunofluorescence staining in NB4 *FASN* depleted cells (Supplementary Figure 2C-D). Of note, at steady state conditions, knocking down *FASN* did not affect proliferation compared to control cells. Knocking down *FASN* in NB4 cells resulted in accelerated differentiation into functional granulocytes compared to the control cells as shown by NBT assays (Figure 3B-C) and by CD11b surface expression analysis (Figure 3D). We then assessed the effects of two pharmacological FASN inhibitors, C75 and Orlistat. We used C75 and Orlistat concentrations that do not induce significant cell death (Supplementary Figure 3A-B) or decrease proliferation (Supplementary figure 3C-D) to avoid non-specific effects. Of note, FASN protein levels in APL cells were not reduced by C75 or Orlistat treatment (Supplementary Figure 3E-F). Unexpectedly, co-treatment of NB4 cells with ATRA and C75 (Figure 3E-G) or Orlistat (Figure 3H-J) did not reproduce the phenotype of the *FASN* knockdown cells. Indeed, cells were differentiating similarly or less compared to control treated cells as demonstrated by NBT assays (Figure 3E-F and Figure 3H-I) and CD11b surface expression (Figure 3G and Figure 3). Therefore, we conclude that the catalytic activity of FASN is not involved in impeding ATRA-mediated differentiation in NB4 cells.

3.5. FASN attenuates autophagy by increasing mTOR activity

FASN has been previously reported to promote carcinogenesis by activating mTOR, a master negative regulator of autophagy, via AKT signaling in hepatocellular carcinoma (Hu *et al*, 2016; Calvisi *et al*, 2011). ATRA treatment in APL also reduces mTOR activity leading to autophagy activation (Isakson *et al*, 2010). We therefore hypothesized that FASN may negatively regulate autophagy via mTOR in APL cells, thereby impeding ATRA-induced differentiation. Therefore, we initially confirmed that FASN expression impacts autophagic activity in our system. Autophagy induction

was determined by quantifying endogenous LC3B dots formation by immunofluorescence microscopy (IF) after ATRA treatment (Klionsky *et al*, 2016). In order to measure autophagic flux, ATRA treatment was performed in the presence or absence of BafA1 (Figure 4A-B) (Klionsky *et al*, 2016). In addition, we looked at the direct consequences of mTOR activity in ULK1 and ATG13 phosphorylation. ULK1 (ATG1), a key autophagy gene of the initiation complex, is inhibited by mTOR-mediated phosphorylation at Ser757, leading to reduced autophagic activity (Figure 4C) (Kim *et al*, 2011). In line with FASN activating mTOR, lowering *FASN* expression by shRNA (Figure 4D) resulted in decreased mTOR phosphorylation at Ser2448 (Figure 4E) and mTOR-mediated downstream phosphorylation of ULK1 at Ser757 (Figure 4F). Elevated ULK1 activity was confirmed by an increase of ATG13 activating phosphorylation at Ser318 (Figure 4G) (Joo *et al*, 2011; Petherick *et al*, 2015). These results suggest that FASN expression promotes mTOR activity, which in turn enhances autophagy inhibition in AML cells.

3.6. FASN expression negatively affects transcription factor EB (TFEB) activation

mTOR phosphorylates the transcription factor EB (TFEB), a master regulator of lysosome biogenesis, leading to the sequestration of TFEB within the cytoplasm and inhibition of its transcriptional activity (Vega-Rubin-de-Celis *et al*, 2017; Peña-Llopis *et al*, 2011; Roczniak-Ferguson *et al*, 2012; Napolitano *et al*, 2018). TFEB is a key transcriptional regulator of more than 500 genes that comprise the CLEAR (Coordinated Lysosomal Expression and Regulation) network of autophagy and lysosomal genes (Supplementary Figure 4A). A recent study demonstrated the key role of TFEB during ATRA induced differentiation (Orfali *et al*, 2019). We therefore investigated the relationship between FASN and CLEAR network gene expression.

Interestingly, the majority of the TFEB downstream targets from the different categories (lysosomal hydrolases and accessory proteins, lysosomal membrane, lysosomal acidification, non-lysosomal proteins involved in lysosomal biogenesis and autophagy) are negatively associated with FASN transcript levels in primary AML patient blasts from TCGA analyzed using the UCSC Xena platform (Goldman *et al*, 2019) and the Blood spot gene expression profiles data base (Bagger *et al*, 2016) (Figure 5A, Supplementary Figures 4B-C Supplementary Table 1-2). Furthermore, analyzing RNA-seq data of NB4 cells treated with ATRA confirmed a reduction of FASN expression paralleled by increased TFEB and TFEB target gene transcript levels (Orfali *et al*, 2019) (Figure 5B). To test if the FASN-mTOR pathway is involved in regulating TFEB activity, we analyzed the cellular localization of TFEB upon ATRA treatment in NB4 control and FASN depleted cells. First, we investigated if TFEB translocates to the nucleus following ATRA treatment and if this translocation is paralleled by an increase in lysosome numbers ($LAMP1^+$ dots), assessed by immunofluorescence microscopy (Supplementary Figure 5A-B). Indeed, ATRA treatment resulted in increased $LAMP1^+$ dot formation and nuclear translocation of TFEB. Interestingly, TFEB nuclear translocation occurs faster in FASN depleted NB4 cells compared to control cells (Figure 5C), consistent with an increase in $LAMP1^+$ dot formation (Figure 5D-E). Furthermore, we treated cells with Acridine Orange to quantify the lysosomal integrity by flow cytometry. Acridine Orange is a cell permeable fluorescent dye that, when excited at 488nm, emits light at 530nm (GREEN) in its monomeric form but shifts its emission to 680nm (RED) when accumulating and precipitating inside lysosomes. Therefore, we measured the RED/GREEN ratio of Acridine Orange stained cells by flow cytometry as previously described (Thomé *et al*, 2016). We found that ATRA treatment shifted the ratio towards the red channel (Supplementary Figure 5C). Reducing FASN expression

further accelerated the increase of RED/GREEN ratio indicating enhanced lysosome biogenesis (Figure 5G-H). These results suggest that FASN expression impairs TFEB translocation to the nucleus and therefore reduces lysosome biogenesis

We then evaluated the effect of FASN expression on the transcription of the following TFEB target genes: *BECN1*, *GABARAP*, *STK4* and *WDR45*. All 4 TFEB targets showed increased expression upon ATRA treatment, in line with previous studies (Orfali *et al*, 2015; Brigger *et al*, 2013, 2014a) (Figure 5I). Knock down of *FASN* led to a further increase in the expression of 3/4 TFEB targets analyzed (Figure 5I). These results suggest that FASN retardation of TFEB translocation to the nucleus attenuates CLEAR network gene transcription.

Then, we tested whether we can obtain similar results by lowering FASN protein levels using EGCG. Using different EGCG concentrations, we found a decrease in mTOR phosphorylation at Ser2448 (Figure 6A), an increase of TFEB translocation to the nucleus (Figure 6B), an increase of $LAMP1^{+}$ vesicles (Supplementary Figure 6A-B) and an increase of the RED/GREEN ratio in Acridine Orange stained cells similar to the results seen in FASN-depleted APL cells (Supplementary Figure 6C-E). In addition, we found an upregulation of 3/4 TFEB target genes in presence of EGCG in line with our FASN knockdown experiments (Figure 6C).

Together, these data suggest that high FASN expression results in lower autophagic activity and decreased lysosomal capacity due to increased mTOR activity causing TFEB inhibition.

3.7. Lowering FASN expression improves ATRA therapy in non-APL AML cell lines by inhibiting the mTOR pathway

Given the fact that APL cells treated with EGCG demonstrated improved response to ATRA therapy, we asked if EGCG can be beneficial to other AML subtypes that are refractory to ATRA treatment. We and others previously demonstrated a positive impact of co-treating HL60 AML cells, a non-APL AML cell line that responds to ATRA, with EGCG and ATRA (Britschgi *et al*, 2010; Moradzadeh *et al*, 2018; Lung *et al*, 2002). Therefore, we tested if ATRA-refractory AML cell lines with different genetic backgrounds, namely MOLM-13 (FLT3-ITD^{+}) and OCI/AML2 (DNMT3A R635W mutation), would respond to ATRA in combination with EGCG. Both cell lines showed increased granulocytic differentiation upon the combination treatment as shown by CD11b surface expression (Figure 7A-B). In addition, MOLM-13 and OCI/AML2 showed an increase of RED/GREEN ratio when stained with Acridine Orange (Figure 7C-D). Furthermore, co-treatment with ATRA and EGCG led to a decrease in mTOR activity as seen by a decrease in mTOR (Ser2448) and ULK1 (Ser757) phosphorylation. In MOLM-13, it was paralleled by an increase of ATG13 (Ser318) phosphorylation (Figure 7E-F). We further confirmed these data by genetically inhibiting *FASN* in MOLM-13 (Figure 8A) and OCI/AML2 (Figure 8B) cells. Depleting FASN in both cell lines caused an increase of CD11b surface expression after 3 days of ATRA treatment (Figure 8C-D), coupled with an increased RED/GREEN ratio when stained for Acridine Orange (Figure 8E-F) and lower mTOR activity (Figure 8G-H). Interestingly, we found more variation in lysosomal compartment changes between the experimental duplicates upon ATRA when cells were treated with EGCG (Figure 7D and 7F) than in the knockdown cells (Figures 8F and 8H), perhaps reflecting the lower specificity of EGCG.

Together, our data suggest that reducing FASN expression can increase lysosomal biogenesis and improve the differentiation of non-APL AML cells.

Discussion

In this study, we aimed at further dissecting the function of fatty acid synthase in AML cells and, in particular, its potential role in the differentiation of immature AML blasts. We showed that knocking down *FASN* accelerated ATRA-induced differentiation, while inhibition of its enzymatic function by pharmacological inhibitors such as C75 or Orlistat had no effect. Furthermore, we found that FASN expression activates mTOR resulting in sequestration of TFEB to the cytoplasm. Importantly, inhibiting *FASN* expression, in combination with ATRA treatment, improved differentiation therapy in non-APL AML cells.

Several studies demonstrated a tumor suppressor role of autophagy in AML cells. Autophagy can support degradation of leukemic oncogenes in AML such as FLT3-ITD and PML-RARA (Larrue *et al*, 2016; Rudat *et al*, 2018; Isakson *et al*, 2010). Furthermore, activation of mTORC1 is crucial for leukemia cell proliferation at least partially due to its inhibitory effect on autophagy (Hoshii *et al*, 2012; Watson *et al*, 2015). Accordingly, inhibition of autophagy leads to acceleration of MLL-ENL AML leukemia progression *in vivo* (Watson *et al*, 2015). Our results indicate that increased FASN expression might be a key activator of mTORC1 in AML. Surprisingly, we found that reducing FASN protein levels, but not inhibition of catalytic function, promotes ATRA-induced differentiation. Recently, Bueno *et al.* demonstrated that FASN is key during the transformation from 2- to 3-dimensional growth of cancer cells. This transformation step does not depend on the FASN biosynthetic products palmitate, further hinting to important non-catalytic functions of FASN in carcinogenesis (Bueno *et al*, 2019). Further studies on the interplay between FASN, mTOR and autophagy in AML transformation, progression and therapy resistance are

warranted to improve our understanding of cell fate decisions and could potentially open new avenues to tackle this disease with improved differentiation therapies.

We further confirmed that EGCG positively impacts on cellular differentiation in additional AML subtypes *in vitro* (Britschgi *et al*, 2010; Moradzadeh *et al*, 2018; Lung *et al*, 2002). Searching for potential mediators of the positive effects of EGCG observed during ATRA-induced differentiation, we previously found that EGCG induces expression of the Ca^{2+}/calmodulin-regulated serine/threonine kinase DAPK2. DAPK2 plays a major role in granulocytic differentiation and decreased DAPK2 expression in APL cells can be restored by ATRA and EGCG treatment (Rizzi *et al*, 2007; Britschgi *et al*, 2010; Humbert *et al*, 2017). DAPK2 also negatively regulates mTOR via phosphorylation of raptor at Ser721 as shown in HeLa cells (Ber *et al*, 2015). Therefore, a potential impact of FASN on DAPK2 activity in a leukemic context warrants further investigation.

Interestingly, treating APL cells with ATRA had a negative effect on FASN protein levels (Figure 1C), and we demonstrated that ATRA-induced autophagy contributes to FASN protein degradation. Furthermore, FASN reduction led to increased lysosomal biogenesis suggesting a negative feedback loop between autophagy and FASN. It is reasonable to hypothesize that the more AML cells differentiate the more they become competent to degrade long-lived proteins including FASN. In addition, inhibiting mTOR using Rapamycin or Everolimus accelerates differentiation of APL cells (Jin *et al*, 2018; Isakson *et al*, 2010). While PI3K/AKT/mTOR pathways are activated in about 80% of AML cases, mTOR inhibitors had only modest effects in AML therapy (Mirabilii *et al*, 2018; Tabe *et al*, 2017). Furthermore, despite its role in leukemia cells, mTOR activity is crucial for hematopoietic stem cell (HSC) proliferation and self-renewal potential (Ghosh & Kapur, 2016). Therefore, targeting

FASN with low expression in healthy progenitor cells would allow activation of autophagy in AML cells sparing healthy HSC cells in the bone marrow. In our hands, EGCG treatment only demonstrated partial effects regarding improved differentiation when compared to knocking down FASN in non-APL AML cells. Therefore, a more specific FASN expression inhibitor is needed to improve differentiation therapy in non-APL AML patients.

Indeed, it would be of interest to study the transcriptional regulation of FASN to influence its expression in autophagy deficient cells. Consistently, there are several studies showing that *FASN* transcription is positively affected by retinoic acids (Roder *et al*, 1996; Roder & Schweizer, 2007). However, transcription induction is not mediated by a classic retinoic acid responsive element (RARE) but rather by indirect influence of retinoic acid via *cis*-regulatory elements. Since this involves different cofactors it is tempting to speculate that transcriptional activation might switch to repression depending on the cellular context including specific retinoid-binding proteins and cofactors. We previously found that members of the KLF transcription factor family are often deregulated in primary AML patient samples. Among the different KLF family members downregulated in AML, particularly *KLF5* turned out to be essential for granulocytic differentiation (Humbert *et al*, 2011; Diakiw *et al*, 2012; Li *et al*, 2019). KLF5 forms a transcriptionally active complex with RAR/RXR heterodimers (Lv *et al*, 2013; Kada *et al*, 2008). Interestingly, ectopic expression of KLF5 in U937 non-APL AML cell line was sufficient to significantly increase ATRA-induced differentiation (Shahrin *et al*, 2016). We hypothesize that KLF5 negatively regulates *FASN* transcription in AML cells via the RAR/RXR complex.

In summary, our data suggest that inducing FASN protein degradation is likely to be beneficial for differentiation therapy of non-APL AML cells as this will impede mTOR

and promote TFEB transcriptional activity and autophagy. Furthermore, high FASN expression in AML is partially based on attenuated autophagy activity in this disease.

Acknowledgments

Deborah Shan-Krauer is gratefully acknowledged for excellent technical support. We thank Dr. MS Soengas for providing a mCherry-LC3B lentiviral vector. This study was supported by grants from Swiss Cancer Research (KFS-3409-02-2014 to MPT, MD-PhD 03/17 Scholarship to KS), the Swiss National Science Foundation (31003A_173219 to MPT), the Berne University Research Foundation (45/2018, to MPT), the University of Bern initiator grant, the Bernese Cancer League, “Stiftung für klinisch-experimentelle Tumorforschung”, and the Werner and Hedy Berger-Janser Foundation for Cancer Research (to MH). SMCK is supported by Breakthrough Cancer Research.

Author Contribution

MH, KS, SM, and VR performed the experimental research. MH, KS, SMCK and MPT drafted the article. MH designed the project. MPT gave final approval of the submitted manuscript.

Conflict of interest

None

References

Alo PL, Visca P, Marci A, Mangoni A, Botti C & Di Tondo U (1996) Expression of fatty acid synthase (FAS) as a predictor of recurrence in stage I breast carcinoma patients. *Cancer* **77:** 474–482

Altucci L & Gronemeyer H (2001) The promise of retinoids to fight against cancer. *Nat. Rev. Cancer* **1:** 181–193

505 Asturias FJ, Chadick JZ, Cheung IK, Stark H, Witkowski A, Joshi AK & Smith S
506 (2005) Structure and molecular organization of mammalian fatty acid synthase. *Nat.*
507 *Struct. Mol. Biol.* **12:** 225–232

508 Bagger FO, Sasivarevic D, Sohi SH, Laursen LG, Pundhir S, Sønderby CK, Winther
509 O, Rapin N & Porse BT (2016) BloodSpot: a database of gene expression profiles
510 and transcriptional programs for healthy and malignant haematopoiesis. *Nucleic*
511 *Acids Res.* **44:** D917–D924

512 Bandyopadhyay S, Pai SK, Watabe M, Gross SC, Hirota S, Hosobe S, Tsukada T,
513 Miura K, Saito K, Markwell SJ, Wang Y, Huggenvik J, Pauza ME, Iiizumi M & Watabe
514 K (2005) FAS expression inversely correlates with PTEN level in prostate cancer and
515 a PI 3-kinase inhibitor synergizes with FAS siRNA to induce apoptosis. *Oncogene*
516 **24:** 5389–5395

517 Ber Y, Shiloh R, Gilad Y, Degani N, Bialik S & Kimchi A (2015) DAPK2 is a novel
518 regulator of mTORC1 activity and autophagy. *Cell Death Differ.* **22:** 465–475

519 Brigger D, Proikas-Cezanne T & Tschan MP (2014a) WIPI-dependent autophagy
520 during neutrophil differentiation of NB4 acute promyelocytic leukemia cells. *Cell*
521 *Death Dis.* **5:** e1315–e1315

522 Brigger D, Proikas-Cezanne T & Tschan MP (2014b) WIPI-dependent autophagy
523 during neutrophil differentiation of NB4 acute promyelocytic leukemia cells. *Cell*
524 *Death Dis.* **5:** e1315

525 Brigger D, Torbett BE, Chen J, Fey MF & Tschan MP (2013) Inhibition of GATE-16
526 attenuates ATRA-induced neutrophil differentiation of APL cells and interferes with
527 autophagosome formation. *Biochem. Biophys. Res. Commun.* **438:** 283–288

528 Britschgi A, Simon H-U, Tobler A, Fey MF & Tschan MP (2010) Epigallocatechin-3-
529 gallate induces cell death in acute myeloid leukaemia cells and supports all-trans
530 retinoic acid-induced neutrophil differentiation via death-associated protein kinase 2.
531 *Br. J. Haematol.* **149:** 55–64

532 Bueno MJ, Jimenez-Renard V, Samino S, Capellades J, Junza A, López-Rodríguez
533 ML, Garcia-Carceles J, Lopez-Fabuel I, Bolaños JP, Chandel NS, Yanes O, Colomer
534 R & Quintela-Fandino M (2019) Essentiality of fatty acid synthase in the 2D to

anchorage-independent growth transition in transforming cells. *Nat. Commun.* **10:** 5011

Bullinger L, Schlenk RF, Götz M, Botzenhardt U, Hofmann S, Russ AC, Babiak A, Zhang L, Schneider V, Döhner K, Schmitt M, Döhner H & Greiner J (2013) PRAME-induced inhibition of retinoic acid receptor signaling-mediated differentiation--a possible target for ATRA response in AML without t(15;17). *Clin. Cancer Res. Off. J. Am. Assoc. Cancer Res.* **19:** 2562–2571

Calvisi DF, Wang C, Ho C, Ladu S, Lee SA, Mattu S, Destefanis G, Delogu S, Zimmermann A, Ericsson J, Brozzetti S, Staniscia T, Chen X, Dombrowski F & Evert M (2011) Increased lipogenesis, induced by AKT-mTORC1-RPS6 signaling, promotes development of human hepatocellular carcinoma. *Gastroenterology* **140:** 1071–1083

Dengjel J, Høyer-Hansen M, Nielsen MO, Eisenberg T, Harder LM, Schandorff S, Farkas T, Kirkegaard T, Becker AC, Schroeder S, Vanselow K, Lundberg E, Nielsen MM, Kristensen AR, Akimov V, Bunkenborg J, Madeo F, Jäättelä M & Andersen JS (2012) Identification of Autophagosome-associated Proteins and Regulators by Quantitative Proteomic Analysis and Genetic Screens. *Mol. Cell. Proteomics MCP* **11:** Available at: https://www.ncbi.nlm.nih.gov/pmc/articles/PMC3316729/ [Accessed January 14, 2020]

Diakiw SM, Kok CH, To LB, Lewis ID, Brown AL & D'Andrea RJ (2012) The granulocyte-associated transcription factor Krüppel-like factor 5 is silenced by hypermethylation in acute myeloid leukemia. *Leuk. Res.* **36:** 110–116

Diaz-Blanco E, Bruns I, Neumann F, Fischer JC, Graef T, Rosskopf M, Brors B, Pechtel S, Bork S, Koch A, Baer A, Rohr U-P, Kobbe G, von Haeseler A, Gattermann N, Haas R & Kronenwett R (2007) Molecular signature of CD34(+) hematopoietic stem and progenitor cells of patients with CML in chronic phase. *Leukemia* **21:** 494–504

Feng Y, He D, Yao Z & Klionsky DJ (2014) The machinery of macroautophagy. *Cell Res.* **24:** 24–41

564 Germain P, Chambon P, Eichele G, Evans RM, Lazar MA, Leid M, De Lera AR,
565 Lotan R, Mangelsdorf DJ & Gronemeyer H (2006) International Union of
566 Pharmacology. LX. Retinoic acid receptors. *Pharmacol. Rev.* **58:** 712–725

567 Ghosh J & Kapur R (2016) Regulation of Hematopoietic Stem Cell Self-Renewal and
568 Leukemia Maintenance by the PI3K-mTORC1 Pathway. *Curr. Stem Cell Rep.* **2:**
569 368–378

570 Goldman M, Craft B, Hastie M, Repečka K, McDade F, Kamath A, Banerjee A, Luo
571 Y, Rogers D, Brooks AN, Zhu J & Haussler D (2019) The UCSC Xena platform for
572 public and private cancer genomics data visualization and interpretation. *bioRxiv***:**
573 326470

574 Gump JM & Thorburn A (2014) Sorting cells for basal and induced autophagic flux by
575 quantitative ratiometric flow cytometry. *Autophagy* **10:** 1327–1334

576 Han Jung-Kyu, Lee Hyun-Sook, Yang Han-Mo, Hur Jin, Jun Soo-In, Kim Ju-Young,
577 Cho Chung-Hyun, Koh Gou-Young, Peters Jeffrey M., Park Kyung-Woo, Cho Hyun-
578 Jai, Lee Hae-Young, Kang Hyun-Jae, Oh Byung-Hee, Park Young-Bae & Kim Hyo-
579 Soo (2008) Peroxisome Proliferator–Activated Receptor-δ Agonist Enhances
580 Vasculogenesis by Regulating Endothelial Progenitor Cells Through Genomic and
581 Nongenomic Activations of the Phosphatidylinositol 3-Kinase/Akt Pathway.
582 *Circulation* **118:** 1021–1033

583 Hoshii T, Tadokoro Y, Naka K, Ooshio T, Muraguchi T, Sugiyama N, Soga T, Araki K,
584 Yamamura K & Hirao A (2012) mTORC1 is essential for leukemia propagation but
585 not stem cell self-renewal. *J. Clin. Invest.* **122:** 2114–2129

586 Hu J, Che L, Li L, Pilo MG, Cigliano A, Ribback S, Li X, Latte G, Mela M, Evert M,
587 Dombrowski F, Zheng G, Chen X & Calvisi DF (2016) Co-activation of AKT and c-
588 Met triggers rapid hepatocellular carcinoma development via the mTORC1/FASN
589 pathway in mice. *Sci. Rep.* **6:** 20484

590 Humbert M, Federzoni EA & Tschan MP (2017) Distinct TP73-DAPK2-ATG5 pathway
591 involvement in ATO-mediated cell death versus ATRA-mediated autophagy
592 responses in APL. *J. Leukoc. Biol.* **102:** 1357–1370

593 Humbert M, Halter V, Shan D, Laedrach J, Leibundgut EO, Baerlocher GM, Tobler A,
594 Fey MF & Tschan MP (2011) Deregulated expression of Kruppel-like factors in acute
595 myeloid leukemia. *Leuk. Res.* **35:** 909–913

596 Isakson P, Bjørås M, Bøe SO & Simonsen A (2010) Autophagy contributes to
597 therapy-induced degradation of the PML/RARA oncoprotein. *Blood* **116:** 2324–2331

598 Jin J, Britschgi A, Schläfli AM, Humbert M, Shan-Krauer D, Batliner J, Federzoni EA,
599 Ernst M, Torbett BE, Yousefi S, Simon H-U & Tschan MP (2018) Low Autophagy
600 (ATG) Gene Expression Is Associated with an Immature AML Blast Cell Phenotype
601 and Can Be Restored during AML Differentiation Therapy. *Oxid. Med. Cell. Longev.*
602 **2018:** 1482795

603 Joo JH, Dorsey FC, Joshi A, Hennessy-Walters KM, Rose KL, McCastlain K, Zhang
604 J, Iyengar R, Jung CH, Suen D-F, Steeves MA, Yang C-Y, Prater SM, Kim D-H,
605 Thompson CB, Youle RJ, Ney PA, Cleveland JL & Kundu M (2011) Hsp90-Cdc37
606 Chaperone Complex Regulates Ulk1- and Atg13-Mediated Mitophagy. *Mol. Cell* **43:**
607 572–585

608 Kada N, Suzuki T, Aizawa K, Munemasa Y, Matsumura T, Sawaki D & Nagai R
609 (2008) Acyclic retinoid inhibits functional interaction of transcription factors Krüppel-
610 like factor 5 and retinoic acid receptor-alpha. *FEBS Lett.* **582:** 1755–1760

611 Kang K, Reilly SM, Karabacak V, Gangl MR, Fitzgerald K, Hatano B & Lee C-H
612 (2008) Adipocyte-Derived Th2 Cytokines and Myeloid PPARδ Regulate Macrophage
613 Polarization and Insulin Sensitivity. *Cell Metab.* **7:** 485–495

614 Kim J, Kundu M, Viollet B & Guan K-L (2011) AMPK and mTOR regulate autophagy
615 through direct phosphorylation of Ulk1. *Nat. Cell Biol.* **13:** 132–141

616 Klionsky DJ, Abdelmohsen K, Abe A, Abedin MJ, Abeliovich H, Acevedo Arozena A,
617 Adachi H, Adams CM, Adams PD, Adeli K, Adhihetty PJ, Adler SG, Agam G, Agarwal
618 R, Aghi MK, Agnello M, Agostinis P, Aguilar PV, Aguirre-Ghiso J, Airoldi EM, et al
619 (2016) Guidelines for the use and interpretation of assays for monitoring autophagy
620 (3rd edition). *Autophagy* **12:** 1–222

621 Larrue C, Saland E, Boutzen H, Vergez F, David M, Joffre C, Hospital M-A,
622 Tamburini J, Delabesse E, Manenti S, Sarry JE & Récher C (2016) Proteasome

inhibitors induce FLT3-ITD degradation through autophagy in AML cells. *Blood* **127:** 882–892

Lee C-H, Chawla A, Urbiztondo N, Liao D, Boisvert WA & Evans RM (2003) Transcriptional Repression of Atherogenic Inflammation: Modulation by PPARδ. *Science* **302:** 453–457

Li C, Yan H, Yin J, Ma J, Liao A, Yang S, Wang L, Huang Y, Lin C, Dong Z, Yang B, Cao T, Liu G & Wang L (2019) MicroRNA-21 promotes proliferation in acute myeloid leukemia by targeting Krüppel-like factor 5. *Oncol. Lett.* **18:** 3367–3372

Lung HL, Ip WK, Wong CK, Mak NK, Chen ZY & Leung KN (2002) Anti-proliferative and differentiation-inducing activities of the green tea catechin epigallocatechin-3-gallate (EGCG) on the human eosinophilic leukemia EoL-1 cell line. *Life Sci.* **72:** 257–268

Lv X-R, Zheng B, Li S-Y, Han A-L, Wang C, Shi J-H, Zhang X-H, Liu Y, Li Y-H & Wen J-K (2013) Synthetic retinoid Am80 up-regulates apelin expression by promoting interaction of RARα with KLF5 and Sp1 in vascular smooth muscle cells. *Biochem. J.* **456:** 35–46

Maier T, Jenni S & Ban N (2006) Architecture of mammalian fatty acid synthase at 4.5 \AA resolution. *Science* **311:** 1258–1262

Maningat PD, Sen P, Rijnkels M, Sunehag AL, Hadsell DL, Bray M & Haymond MW (2009) Gene expression in the human mammary epithelium during lactation: the milk fat globule transcriptome. *Physiol. Genomics* **37:** 12–22

Marchwicka A, Cebrat M, Sampath P, Śnieżewski Ł & Marcinkowska E (2014) Perspectives of Differentiation Therapies of Acute Myeloid Leukemia: The Search for the Molecular Basis of Patients' Variable Responses to 1,25-Dihydroxyvitamin D and Vitamin D Analogs. *Front. Oncol.* **4:** Available at: http://www.ncbi.nlm.nih.gov/pmc/articles/PMC4034350/ [Accessed February 1, 2016]

Mirabilii S, Ricciardi MR, Piedimonte M, Gianfelici V, Bianchi MP & Tafuri A (2018) Biological Aspects of mTOR in Leukemia. *Int. J. Mol. Sci.* **19:** Available at: https://www.ncbi.nlm.nih.gov/pmc/articles/PMC6121663/ [Accessed August 30, 2019]

652 Moradzadeh M, Roustazadeh A, Tabarraei A, Erfanian S & Sahebkar A (2018)
653 Epigallocatechin-3-gallate enhances differentiation of acute promyelocytic leukemia
654 cells via inhibition of PML-RARα and HDAC1. *Phytother. Res. PTR* **32:** 471–479

655 Napolitano G, Esposito A, Choi H, Matarese M, Benedetti V, Malta CD, Monfregola J,
656 Medina DL, Lippincott-Schwartz J & Ballabio A (2018) mTOR-dependent
657 phosphorylation controls TFEB nuclear export. *Nat. Commun.* **9:** 3312

658 Odegaard JI, Ricardo-Gonzalez RR, Red Eagle A, Vats D, Morel CR, Goforth MH,
659 Subramanian V, Mukundan L, Ferrante AW & Chawla A (2008) Alternative M2
660 Activation of Kupffer Cells by PPARδ Ameliorates Obesity-Induced Insulin
661 Resistance. *Cell Metab.* **7:** 496–507

662 Orfali N, O'Donovan TR, Cahill MR, Benjamin D, Nanus DM, McKenna SL, Gudas LJ
663 & Mongan NP (2019) All-trans retinoic acid (ATRA) induced TFEB expression is
664 required for myeloid differentiation in acute promyelocytic leukemia (APL). *Eur. J.*
665 *Haematol.*

666 Orfali N, O'Donovan TR, Nyhan MJ, Britschgi A, Tschan MP, Cahill MR, Mongan NP,
667 Gudas LJ & McKenna SL (2015) Induction of autophagy is a key component of all-
668 trans-retinoic acid-induced differentiation in leukemia cells and a potential target for
669 pharmacologic modulation. *Exp. Hematol.* **43:** 781-793.e2

670 Park J, Lee SE, Hur J, Hong EB, Choi J-I, Yang J-M, Kim J-Y, Kim Y-C, Cho H-J,
671 Peters JM, Ryoo S-B, Kim YT & Kim H-S (2015) M-CSF from Cancer Cells Induces
672 Fatty Acid Synthase and PPARβ/δ Activation in Tumor Myeloid Cells, Leading to
673 Tumor Progression. *Cell Rep.* **10:** 1614–1625

674 Peña-Llopis S, Vega-Rubin-de-Celis S, Schwartz JC, Wolff NC, Tran TAT, Zou L, Xie
675 X-J, Corey DR & Brugarolas J (2011) Regulation of TFEB and V-ATPases by
676 mTORC1. *EMBO J.* **30:** 3242–3258

677 Peters JM & Gonzalez FJ (2009) Sorting out the functional role(s) of peroxisome
678 proliferator-activated receptor-β/δ (PPARβ/δ) in cell proliferation and cancer.
679 *Biochim. Biophys. Acta BBA - Rev. Cancer* **1796:** 230–241

680 Petherick KJ, Conway OJL, Mpamhanga C, Osborne SA, Kamal A, Saxty B & Ganley
681 IG (2015) Pharmacological Inhibition of ULK1 Kinase Blocks Mammalian Target of
682 Rapamycin (mTOR)-dependent Autophagy. *J. Biol. Chem.* **290:** 11376–11383

683 Petrie K, Zelent A & Waxman S (2009) Differentiation therapy of acute myeloid
684 leukemia: past, present and future. *Curr. Opin. Hematol.* **16:** 84–91

685 Pizer ES, Kurman RJ, Pasternack GR & Kuhajda FP (1997) Expression of fatty acid
686 synthase is closely linked to proliferation and stromal decidualization in cycling
687 endometrium. *Int. J. Gynecol. Pathol. Off. J. Int. Soc. Gynecol. Pathol.* **16:** 45–51

688 Pizer ES, Lax SF, Kuhajda FP, Pasternack GR & Kurman RJ (1998) Fatty acid
689 synthase expression in endometrial carcinoma. *Cancer* **83:** 528–537

690 Poole B & Ohkuma S (1981) Effect of weak bases on the intralysosomal pH in mouse
691 peritoneal macrophages. *J. Cell Biol.* **90:** 665–669

692 Rashid A, Pizer ES, Moga M, Milgraum LZ, Zahurak M, Pasternack GR, Kuhajda FP
693 & Hamilton SR (1997) Elevated expression of fatty acid synthase and fatty acid
694 synthetic activity in colorectal neoplasia. *Am. J. Pathol.* **150:** 201–208

695 Rice AM, Holtz KM, Karp J, Rollins S & Sartorelli AC (2004) Analysis of the
696 relationship between Scl transcription factor complex protein expression patterns and
697 the effects of LiCl on ATRA-induced differentiation in blast cells from patients with
698 acute myeloid leukemia. *Leuk. Res.* **28:** 1227–1237

699 Rizzi M, Tschan MP, Britschgi C, Britschgi A, Hügli B, Grob TJ, Leupin N, Mueller
700 BU, Simon H-U, Ziemiecki A, Torbett BE, Fey MF & Tobler A (2007) The death-
701 associated protein kinase 2 is up-regulated during normal myeloid differentiation and
702 enhances neutrophil maturation in myeloid leukemic cells. *J. Leukoc. Biol.* **81:** 1599–
703 1608

704 Roczniak-Ferguson A, Petit CS, Froehlich F, Qian S, Ky J, Angarola B, Walther TC &
705 Ferguson SM (2012) The transcription factor TFEB links mTORC1 signaling to
706 transcriptional control of lysosome homeostasis. *Sci. Signal.* **5:** ra42

Roder K & Schweizer M (2007) Retinoic acid-mediated transcription and maturation of SREBP-1c regulates fatty acid synthase via cis-elements responsible for nutritional regulation. *Biochem. Soc. Trans.* **35:** 1211–1214

Roder K, Wolf SS & Schweizer M (1996) Regulation of the fatty acid synthase promoter by retinoic acid. *Biochem. Soc. Trans.* **24:** 233S

Rudat S, Pfaus A, Cheng YY, Holtmann J, Ellegast JM, Bühler C, Marcantonio DD, Martinez E, Göllner S, Wickenhauser C, Müller-Tidow C, Lutz C, Bullinger L, Milsom MD, Sykes SM, Fröhling S & Scholl C (2018) RET-mediated autophagy suppression as targetable co-dependence in acute myeloid leukemia. *Leukemia* **32:** 2189–2202

Schenk T, Chen WC, Göllner S, Howell L, Jin L, Hebestreit K, Klein H-U, Popescu AC, Burnett A, Mills K, Casero RA, Marton L, Woster P, Minden MD, Dugas M, Wang JCY, Dick JE, Müller-Tidow C, Petrie K & Zelent A (2012) Inhibition of the LSD1 (KDM1A) demethylase reactivates the all-trans-retinoic acid differentiation pathway in acute myeloid leukemia. *Nat. Med.* **18:** 605–611

Shahrin NH, Diakiw S, Dent LA, Brown AL & D'Andrea RJ (2016) Conditional knockout mice demonstrate function of Klf5 as a myeloid transcription factor. *Blood* **128:** 55–59

Shurbaji MS, Kalbfleisch JH & Thurmond TS (1996) Immunohistochemical detection of a fatty acid synthase (OA-519) as a predictor of progression of prostate cancer. *Hum. Pathol.* **27:** 917–921

Su M, Alonso S, Jones JW, Yu J, Kane MA, Jones RJ & Ghiaur G (2015) All-Trans Retinoic Acid Activity in Acute Myeloid Leukemia: Role of Cytochrome P450 Enzyme Expression by the Microenvironment. *PLOS ONE* **10:** e0127790

Suzuki K, Nakamura S, Morimoto M, Fujii K, Noda NN, Inagaki F & Ohsumi Y (2014) Proteomic Profiling of Autophagosome Cargo in Saccharomyces cerevisiae. *PLOS ONE* **9:** e91651

Tabe Y, Tafuri A, Sekihara K, Yang H & Konopleva M (2017) Inhibition of mTOR kinase as a therapeutic target for acute myeloid leukemia. *Expert Opin. Ther. Targets* **21:** 705–714

736 Thomé MP, Filippi-Chiela EC, Villodre ES, Migliavaca CB, Onzi GR, Felipe KB &
737 Lenz G (2016) Ratiometric analysis of Acridine Orange staining in the study of acidic
738 organelles and autophagy. *J. Cell Sci.* **129:** 4622–4632

739 Tschan MP, Fischer KM, Fung VS, Pirnia F, Borner MM, Fey MF, Tobler A & Torbett
740 BE (2003) Alternative splicing of the human cyclin D-binding Myb-like protein
741 (hDMP1) yields a truncated protein isoform that alters macrophage differentiation
742 patterns. *J. Biol. Chem.* **278:** 42750–42760

743 Vega-Rubin-de-Celis S, Peña-Llopis S, Konda M & Brugarolas J (2017) Multistep
744 regulation of TFEB by MTORC1. *Autophagy* **13:** 464–472

745 Visca P, Sebastiani V, Botti C, Diodoro MG, Lasagni RP, Romagnoli F, Brenna A, De
746 Joannon BC, Donnorso RP, Lombardi G & Alo PL (2004) Fatty acid synthase (FAS)
747 is a marker of increased risk of recurrence in lung carcinoma. *Anticancer Res.* **24:**
748 4169–4173

749 Volpe JJ & Vagelos PR (1976) Mechanisms and regulation of biosynthesis of
750 saturated fatty acids. *Physiol. Rev.* **56:** 339–417

751 Wang Z, Cao L, Kang R, Yang M, Liu L, Zhao Y, Yu Y, Xie M, Yin X, Livesey KM &
752 Tang D (2011) Autophagy regulates myeloid cell differentiation by p62/SQSTM1-
753 mediated degradation of PML-RARα oncoprotein. *Autophagy* **7:** 401–411

754 Wang Z-Y & Chen Z (2008) Acute promyelocytic leukemia: from highly fatal to highly
755 curable. *Blood* **111:** 2505–2515

756 Watson AS, Riffelmacher T, Stranks A, Williams O, De Boer J, Cain K, MacFarlane
757 M, McGouran J, Kessler B, Khandwala S, Chowdhury O, Puleston D, Phadwal K,
758 Mortensen M, Ferguson D, Soilleux E, Woll P, Jacobsen SEW & Simon AK (2015)
759 Autophagy limits proliferation and glycolytic metabolism in acute myeloid leukemia.
760 *Cell Death Discov.* **1:**

761 Weiss L, Hoffmann GE, Schreiber R, Andres H, Fuchs E, Körber E & Kolb HJ (1986)
762 Fatty-acid biosynthesis in man, a pathway of minor importance. Purification, optimal
763 assay conditions, and organ distribution of fatty-acid synthase. *Biol. Chem. Hoppe.*
764 *Seyler* **367:** 905–912

765 Yamamoto A, Tagawa Y, Yoshimori T, Moriyama Y, Masaki R & Tashiro Y (1998)
766 Bafilomycin A1 prevents maturation of autophagic vacuoles by inhibiting fusion
767 between autophagosomes and lysosomes in rat hepatoma cell line, H-4-II-E cells.
768 *Cell Struct. Funct.* **23:** 33–42

769 Yeh CW, Chen WJ, Chiang CT, Lin-Shiau SY & Lin JK (2003) Suppression of fatty
770 acid synthase in MCF-7 breast cancer cells by tea and tea polyphenols: a possible
771 mechanism for their hypolipidemic effects. *Pharmacogenomics J.* **3:** 267

772 Zuo X, Peng Z, Moussalli MJ, Morris JS, Broaddus RR, Fischer SM & Shureiqi I
773 (2009) Targeted Genetic Disruption of Peroxisome Proliferator–Activated Receptor-δ
774 and Colonic Tumorigenesis. *JNCI J. Natl. Cancer Inst.* **101:** 762–767

775

776

Figure Legends

Figure 1: Increased FASN expression is associated with an immature AML blast phenotype.

A. FASN mRNA levels in AML blasts, $CD34^+$ progenitor cells and granulocytes from healthy donors were quantified by qPCR. All the samples were obtained from the Inselspital, Bern, Switzerland. AML patient cells and granulocytes were isolated using Ficoll gradient density centrifugation. Values are the differences in Ct-values between FASN and the housekeeping gene and ABL1. MNW * $p<0.05$, ** $p<0.0$. B. Blood spot data bank analysis of FASN expression in AML blasts compared to granulocytes from healthy donors. MNW * $p<0.05$, ** $p<0.01$. C. Western blot analysis of FASN regulation in NB4 and HT93 APL cells upon ATRA treatment at different time points (1, 2 and 3 days). Total protein was extracted and submitted to immunoblotting using anti-FASN antibody. Total protein is shown as loading control. The relative protein expressions were normalized to total protein and quantified using ImageJ software (NIH, Bethesda, MD, USA). Data are represented as a mean (n=3), Error bars: SD.

Figure 2: FASN is degraded via autophagy. A. NB4 cells were treated with ATRA and three concentrations of Bafilomycin A1 (BafA1) for 24h. NB4 cells were lysed and subjected to western blot analysis as described in 1C. Quantification of the bands was done using ImageJ software. Data are represented as a mean (n=3), Error bars: SD. B. NB4 cells stably expressing mCherry-LC3B were treated with ATRA and different concentrations of Bafilomycin A1 (BafA1) for 24h. NB4 mCherry-LC3B cells were fixed and stained for endogenous FASN. The colocalization analysis was performed using ImageJ software. Scale: 10µm C. NB4 cells were treated as in 2C and fixed and stained for endogenous FASN and p62. The colocalization analysis was performed using ImageJ software. Scale: 10µm. Results shown are from at least

two biological duplicates. (C) EGCG potentiate ATRA-induced FASN degradation by autophagy. (D) FASN and p62 western blot analysis of NB4 cells treated with DMSO (right panel) or ATRA (left panel), in combination with different EGCG (5µM to 15µM) and BafA1 (100nm) concentrations for 24h. Total cell lysates were subjected to western blotting. Quantification of the western blot was done as in Figure 1C.

Figure 3: Reducing FASN protein levels improves ATRA-mediated neutrophil differentiation of APL cells. (A-D). NB4 cells were stably transduced with non-targeting shRNA (SHC002) or shRNAs targeting *FASN* (sh*FASN*_1 and sh*FASN*_2) lentiviral vectors and differentiated with 1µM ATRA for 1, 2 or 3 days. A. FASN western blot analysis of control and sh*FASN* (sh*FASN*_1, _2) expressing NB4 cell populations. B-C. NBT reduction in ATRA-treated NB4 control (SHC002) and *FASN* knockdown (sh*FASN*_1, _2) cells. B. Representative images of NBT assays in control and FASN depleted NB4 cells. C. Quantification of the percentage of NBT^+ cells. D. Flow cytometry analysis of CD11b surface expression NB4 control (SHC002) and *FASN* knockdown (sh*FASN*_1, _2) NB4 cells upon ATRA treatment. E-G. NB4 cells were treated with the indicated C75 concentrations for 3 days in combination with ATRA. E-F. NBT reduction during ATRA-mediated neutrophil differentiation of NB4 control and C75 treated cells. E. Representative images of NBT assays in control and C75 treated NB4 cells upon ATRA-mediated differentiation. F. Quantification of the percentage of NBT^+ cells. G. Flow cytometry analysis of CD11b surface expression in NB4 control and C75 treated cells upon ATRA-mediated differentiation. H-J. NB4 cells were treated with the indicated Orlistat concentrations for 3 days in combination with ATRA. H-I. NBT reduction during ATRA-mediated neutrophil differentiation of NB4 control and Orlistat treated cells. H. Representative images of NBT assays in control and Orlistat treated NB4 cells upon ATRA-mediated differentiation. I. Quantification of the percentage of NBT^+ cells. J. Flow cytometry

analysis of CD11b surface expression in NB4 control and Orlistat treated cells upon ATRA-mediated differentiation. Data are represented as a mean (n=3), Error bars: SD.

Figure 4: FASN expression is linked to increased mTOR activity. A-C. Autophagy induction in NB4 sh*FASN* cells treated with 1µM ATRA for 24h, in the presence or absence of BafA1 during the last 2h before harvesting. A-B. NB4 control (SHC002) and FASN knockdown (sh*FASN*_1, _2) cells were subjected to LC3B immunofluorescence. A. Representative picture of LC3B punctae in NB4 control (SHC002) and FASN knockdown (sh*FASN*_1, _2) cells. Scale: 10µm B. Quantification of autophagy flux. Three independent experiments were quantified as described in (Humbert *et al*, 2017). C. Scheme of mTOR activity on the ULK1 complex D. NB4 control (SHC002) and FASN knockdown (sh*FASN*_1, _2) cells were treated for 1 to 3 days with ATRA. Total protein was extracted and subjected to immunoblotting using anti-FASN, anti-pmTOR(Ser2448), anti- pULK1(Ser757), anti-ULK1, anti-pATG13(Ser318) and anti-ATG13 antibodies. E-F. Relative protein expressions of two independent experiments were normalized to total protein or the respective non-phosphorylated protein and quantified using ImageJ software (NIH, Bethesda, MD, USA). E. pmTOR(Ser2448) normalized to total protein. F. pULK1(Ser757) normalized to total ULK1. G. pATG13(Ser318) normalized to total ATG13. Results shown are from at least two biological duplicates.

Figure 5: FASN expression negatively associates with TFEB activity. A. Heatmaps of the correlation between FASN and TFEB target genes extracted from the TCGA-AML cohort analyzed by the UCSD xena platform and from the bloodspot data bank (Spearman, p values in Supplementary Table1 and 2). B. mRNA sequencing data of NB4 cells treated with ATRA. Relative expression of *FASN*, *TFEB* and TFEB

853 transcriptional targets involved in lysosomal function and biogenesis are shown. C-H.
854 NB4 control (SHC002) and *FASN* knockdown (sh*FASN*_1, _2) cells were treated for
855 1 to 3 days with ATRA. (C) Immunofluorescence microscopy of endogenous TFEB
856 (red) and α-tubulin (green). IgG staining was used as negative control. Nuclei were
857 stained with DAPI (blue). (D) Immunofluorescence microscopy of endogenous
858 LAMP1 (red). Nuclei were stained with DAPI (blue). Scale: 10µm (E) LAMP1 punctae
859 quantification of cells shown in D. Scale: 10µm (F-H) Acridine Orange staining. (F)
860 Histogram representation of the ratio between RED and GREEN of NB4 control
861 (SHC002) cells treated as described in 6C. (G) Representative histogram of NB4
862 control (SHC002) and *FASN* knockdown (sh*FASN*_1, _2) cells treated as in 6C. (H)
863 Overton percentage positive quantification of the RED/GREEN ratio of NB4 control
864 (SHC002) and *FASN* knockdown (sh*FASN*_1, _2) cells treated with ATRA at
865 indicated times. (I) Evaluation of *BECN1*, *GABARAP*, *STK4* and *WDR45* mRNA
866 transcripts was done by qPCR. Values were normalized to the HMBS housekeeping
867 gene. Results shown are from at least two biological duplicates.

868 **Figure 6**: EGCG treatment accelerates TFEB translocation to the nucleus and
869 improves lysosome biogenesis. NB4 and HT93 APL cells were treated for 1 to 3 days
870 with ATRA in combination with indicated concentrations of EGCG. Cells were then
871 subjected to (A) Western blot analysis of FASN and pmTOR(Ser2448), (B) TFEB
872 endogenous immunofluorescence. B. Representative pictures of TFEB in NB4 cells
873 treated with ATRA and different concentrations of EGCG (5µM, 10µM and 15µM),
874 Scale: 10µm. (C) Evaluation of *BECN1*, *GABARAP*, *STK4* and *WDR45* mRNA
875 transcripts was done by qPCR. Values were normalized to the HMBS housekeeping
876 gene. Results shown are from at least two biological duplicates.

Figure 7: Lowering FASN protein expression levels improves ATRA therapy in non-APL AML cells. A-F: MOLM-13 (A, C, E), and OCI-AML2 (B, D, F) cells were treated with ATRA and different concentrations of EGCG (5µM, 10µM and 15µM) for 3 days (n=3). (A-B) CD11b surface staining was analyzed by flow cytometry. Box blot represent the median fluorescence intensity (MFI) of CD11b positive cells. C-D. Acridine Orange staining. Analysis was performed as in Figure 6E-G. E-F. Total protein extracted from MOLM-13 and OCI-AML2 cells treated as in 7A/B were subjected to immunoblotting using anti-FASN, anti-pmTOR(Ser2448), anti-pULK1(Ser757), anti-ULK1, anti-pATG13(Ser318) and anti-ATG13 antibodies. Results shown are from at least two biological duplicates.

Figure 8: MOLM-13 and OCI/AML2 were stably transduced with 2 independent shRNA targeting *FASN* (n=3) A-B.: *FASN* knockdown efficiency was validated in MOLM-13 (A) and OCI/AML2 (B) by western blotting. C-H. MOLM-13 and OCI/AML2 control and FASN knockdown cells were treated with ATRA for 3 days. (C-D) CD11b surface marker expression was analyzed as in A-B. (E-F) Acridine Orange staining analysis was performed as in 7E-G. (G-H) Western blot analysis of total protein was extracted and subjected to immunoblotting using anti-FASN, anti-pmTOR(Ser2448), anti- pULK1(Ser757), anti-ULK1, anti-pATG13(Ser318) and anti-ATG13 antibodies. Results shown are from at least two biological duplicates.

Figure 1

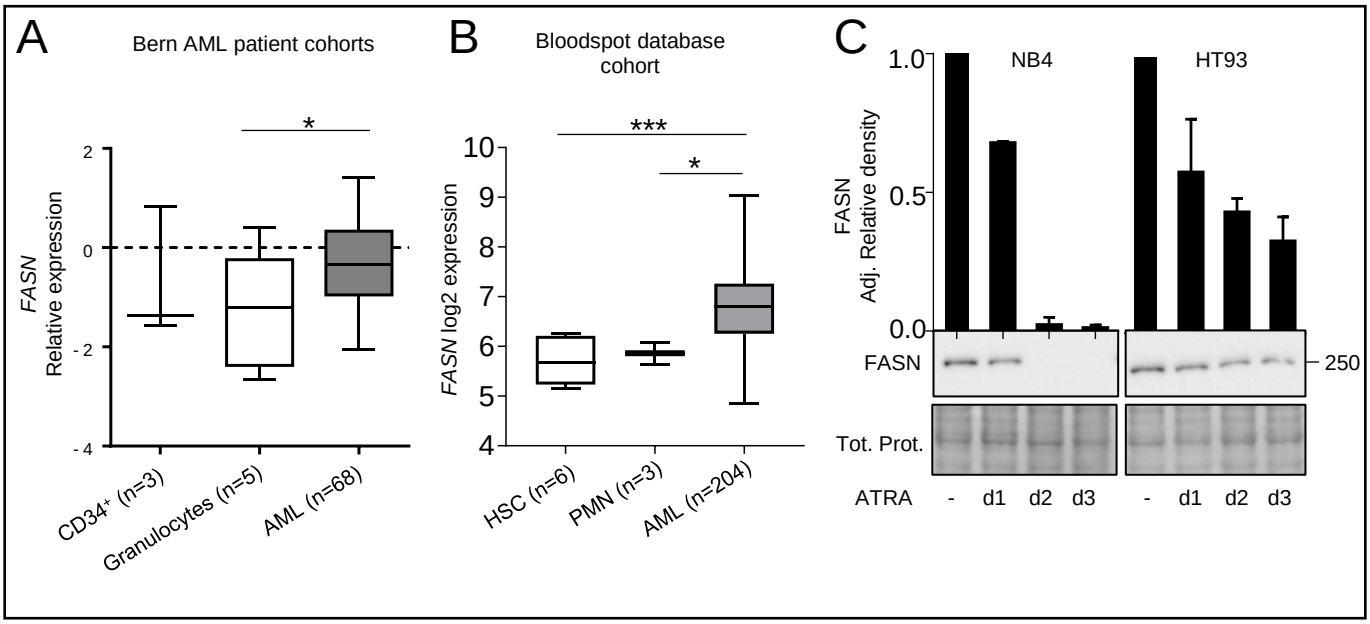
A
Bern AML patient cohorts
FASN Relative expression
2
0
- 2
- 4
*
CD34+ (n=3)
Granulocytes (n=5)
AML (n=68)
B
Bloodspot database cohort
FASN log2 expression
10
9
8
7
6
5
4
***
*
HSC (n=6)
PMN (n=3)
AML (n=204)
C
NB4
HT93
FASN Adj. Relative density
1.0
0.5
0.0
FASN
250
Tot. Prot.
ATRA
-
d1
d2
d3
-
d1
d2
d3

Figure 2

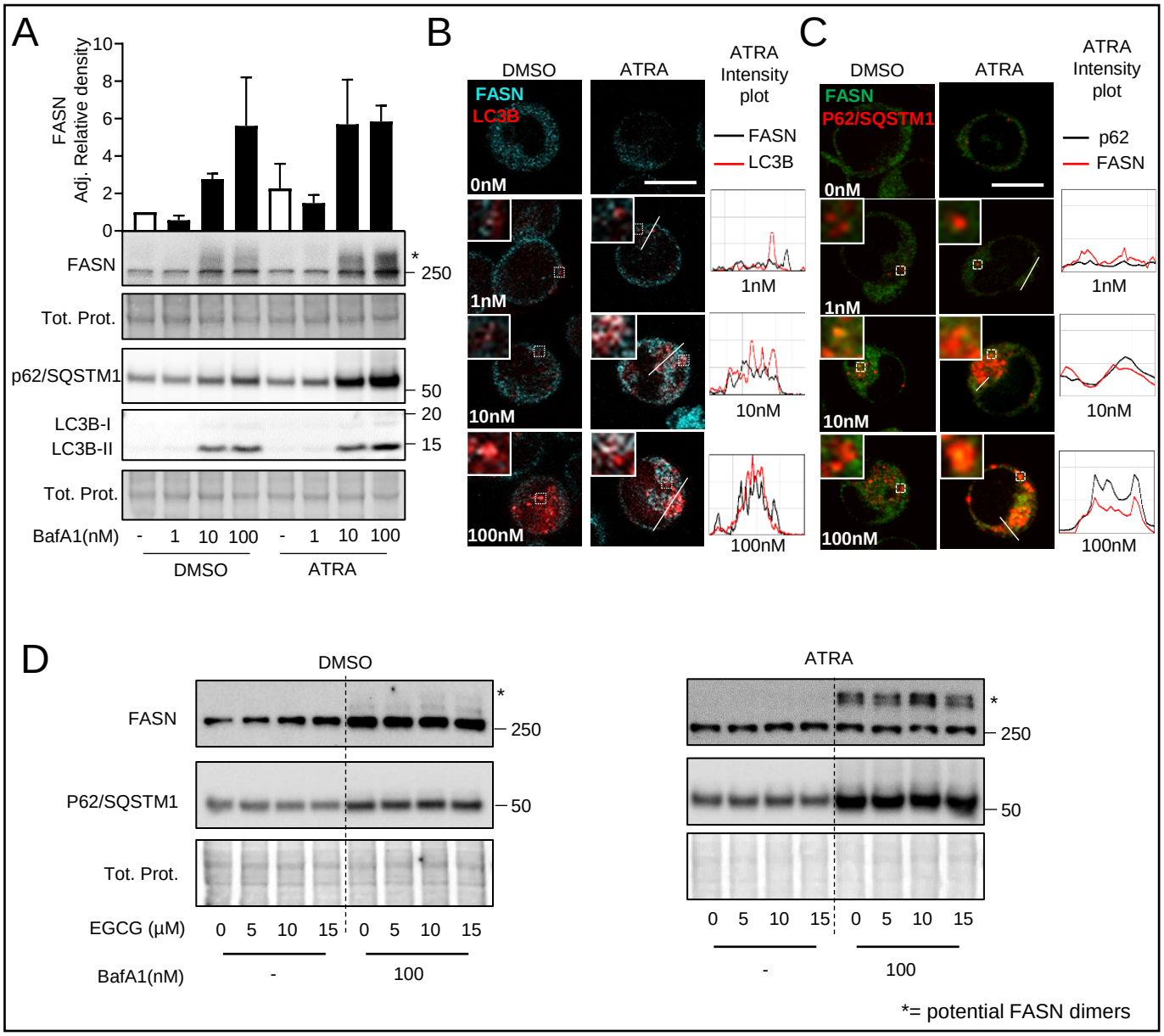
A
FASN Adj. Relative density
10
8
6
4
2
0
FASN
Tot. Prot.
p62/SQSTM1
LC3B-I
LC3B-II
Tot. Prot.
*
250
50
20
15
BafA1(nM) - 1 10 100 - 1 10 100
DMSO
ATRA
B
DMSO
ATRA
ATRA Intensity plot
FASN
LC3B
0nM
1nM
10nM
100nM
C
DMSO
ATRA
ATRA Intensity plot
FASN
P62/SQSTM1
p62
FASN
0nM
1nM
10nM
100nM
D
DMSO
ATRA
FASN
P62/SQSTM1
Tot. Prot.
*
250
50
EGCG (µM) 0 5 10 15 0 5 10 15
BafA1(nM) - 100
*= potential FASN dimers

Figure 3

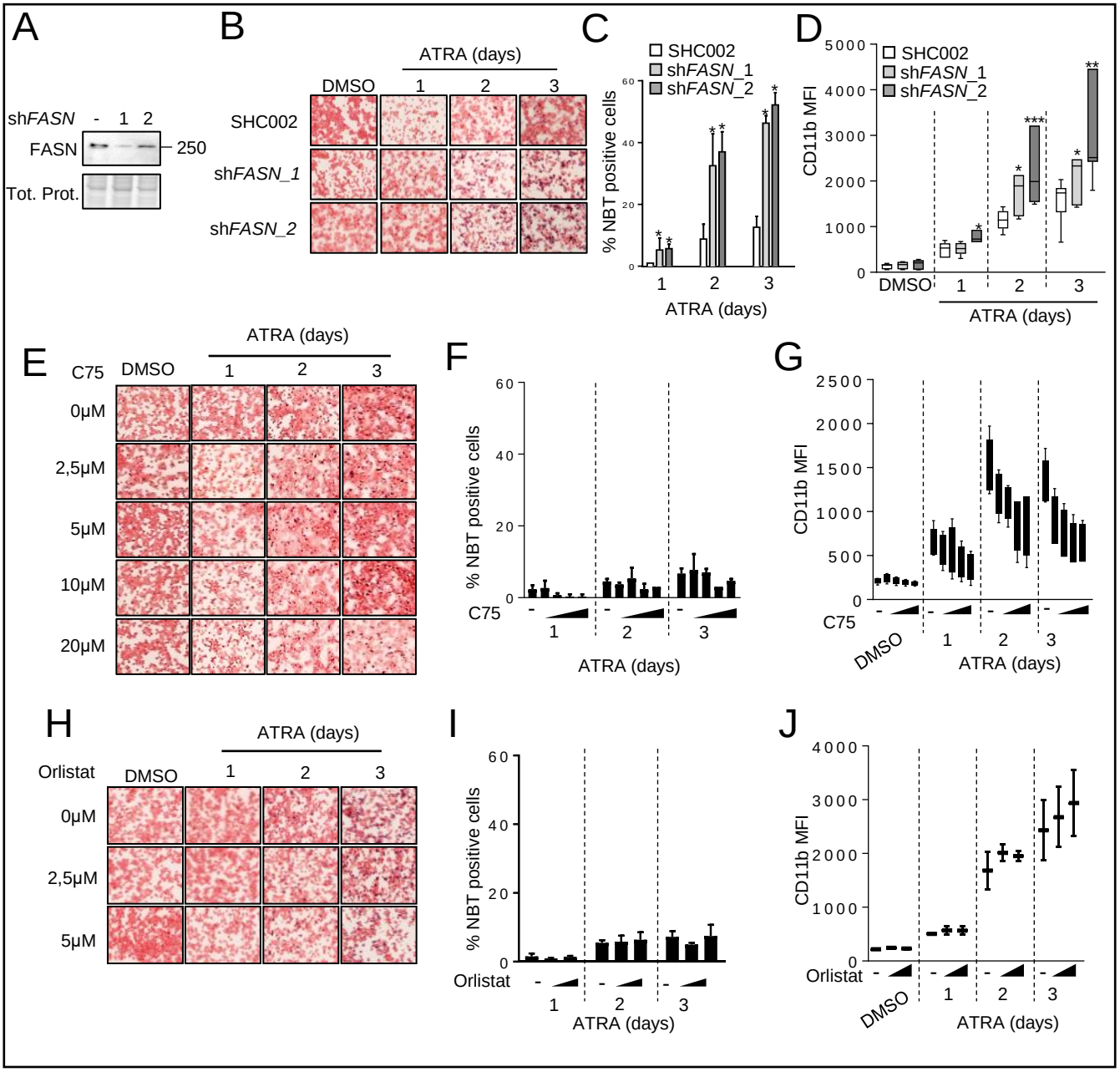
A
shFASN - 1 2
FASN
250
Tot. Prot.
B
ATRA (days)
DMSO 1 2 3
SHC002
shFASN_1
shFASN_2
C
SHC002
shFASN_1
shFASN_2
% NBT positive cells
ATRA (days)
D
SHC002
shFASN_1
shFASN_2
CD11b MFI
DMSO 1 2 3
ATRA (days)
E
C75
ATRA (days)
DMSO 1 2 3
0μM
2,5μM
5μM
10μM
20μM
F
% NBT positive cells
C75
ATRA (days)
G
CD11b MFI
C75
DMSO 1 2 3
ATRA (days)
H
Orlistat
ATRA (days)
DMSO 1 2 3
0μM
2,5μM
5μM
I
% NBT positive cells
Orlistat
ATRA (days)
J
CD11b MFI
Orlistat
DMSO 1 2 3
ATRA (days)

Figure 4

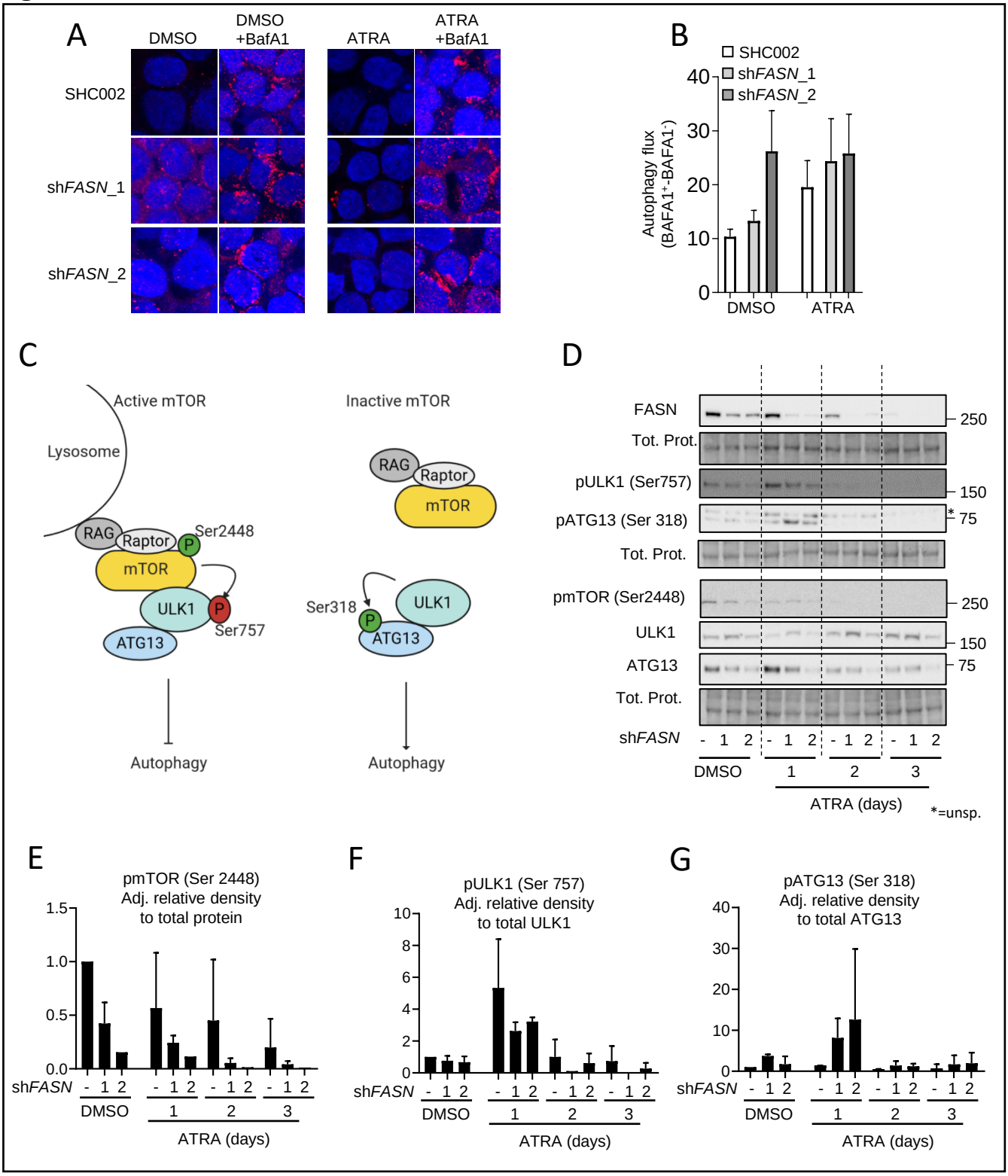
A
DMSO
DMSO +BafA1
ATRA
ATRA +BafA1
SHC002
shFASN_1
shFASN_2
B
SHC002
shFASN_1
shFASN_2
Autophagy flux (BAFA1+-BAFA1-)
40
30
20
10
0
DMSO
ATRA
C
Active mTOR
Lysosome
RAG
Raptor
P
Ser2448
mTOR
ULK1
P
Ser757
ATG13
Autophagy
Inactive mTOR
RAG
Raptor
mTOR
Ser318
P
ULK1
ATG13
Autophagy
D
FASN
Tot. Prot.
pULK1 (Ser757)
pATG13 (Ser 318)
Tot. Prot.
pmTOR (Ser2448)
ULK1
ATG13
Tot. Prot.
250
150
75
*
250
150
75
shFASN - 1 2 - 1 2 - 1 2 - 1 2
DMSO
1
2
3
ATRA (days)
*=unsp.
E
pmTOR (Ser 2448)
Adj. relative density
to total protein
1.5
1.0
0.5
0.0
shFASN - 1 2 - 1 2 - 1 2 - 1 2
DMSO
1
2
3
ATRA (days)
F
pULK1 (Ser 757)
Adj. relative density
to total ULK1
10
8
6
4
2
0
shFASN - 1 2 - 1 2 - 1 2 - 1 2
DMSO
1
2
3
ATRA (days)
G
pATG13 (Ser 318)
Adj. relative density
to total ATG13
40
30
20
10
0
shFASN - 1 2 - 1 2 - 1 2 - 1 2
DMSO
1
2
3
ATRA (days)

Figure 5

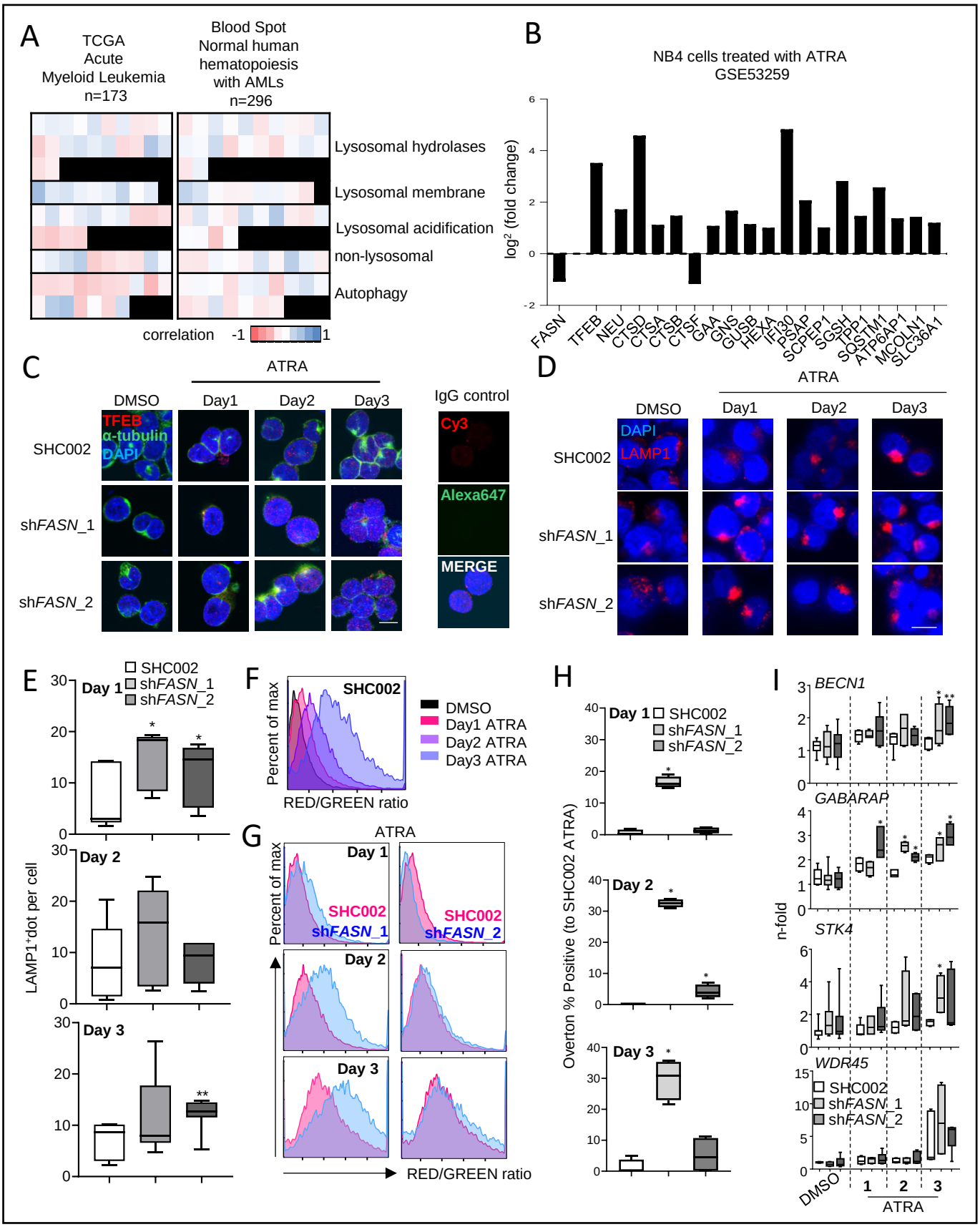
A
TCGA Acute Myeloid Leukemia n=173
Blood Spot Normal human hematopoiesis with AMLs n=296
Lysosomal hydrolases
Lysosomal membrane
Lysosomal acidification
non-lysosomal
Autophagy
correlation -1 1
B
NB4 cells treated with ATRA GSE53259
log2 (fold change)
FASN TFEB NEU CTSD CTSA CTSB CTSF GAA GNS GUSB HEXA IFI30 PSAP SCPEP1 SGSH TPP1 SQSTM1 ATP6AP1 MCOLN1 SLC36A1
C
ATRA
DMSO Day1 Day2 Day3
IgG control
SHC002
shFASN_1
shFASN_2
TFEB
α-tubulin
DAPI
Cy3
Alexa647
MERGE
D
ATRA
DMSO Day1 Day2 Day3
SHC002
shFASN_1
shFASN_2
DAPI
LAMP1
E
SHC002
shFASN_1
shFASN_2
Day 1
Day 2
Day 3
LAMP1+dot per cell
F
SHC002
Percent of max
RED/GREEN ratio
DMSO
Day1 ATRA
Day2 ATRA
Day3 ATRA
G
ATRA
Day 1
Day 2
Day 3
SHC002
shFASN_1
SHC002
shFASN_2
Percent of max
RED/GREEN ratio
H
Day 1
Day 2
Day 3
SHC002
shFASN_1
shFASN_2
Overton % Positive (to SHC002 ATRA)
I
BECN1
GABARAP
STK4
WDR45
SHC002
shFASN_1
shFASN_2
n-fold
DMSO
1
2
3
ATRA

Figure 6

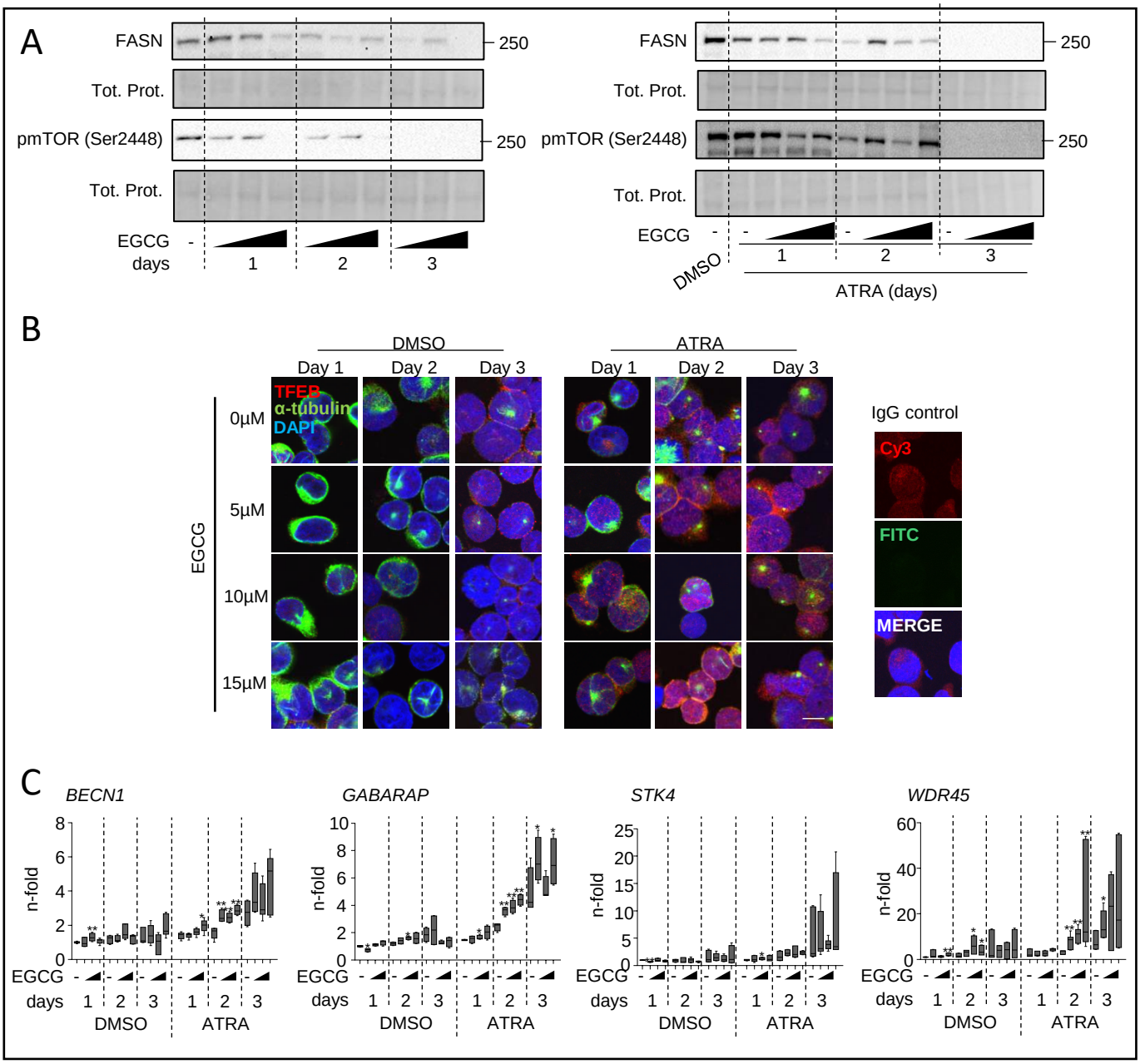
A
FASN
Tot. Prot.
pmTOR (Ser2448)
Tot. Prot.
250
250
EGCG
days
1
2
3
DMSO
ATRA (days)
B
DMSO
ATRA
Day 1
Day 2
Day 3
TFEB
α-tubulin
DAPI
EGCG
0μM
5μM
10μM
15μM
IgG control
Cy3
FITC
MERGE
C
BECN1
GABARAP
STK4
WDR45
n-fold
DMSO
ATRA

Figure 7

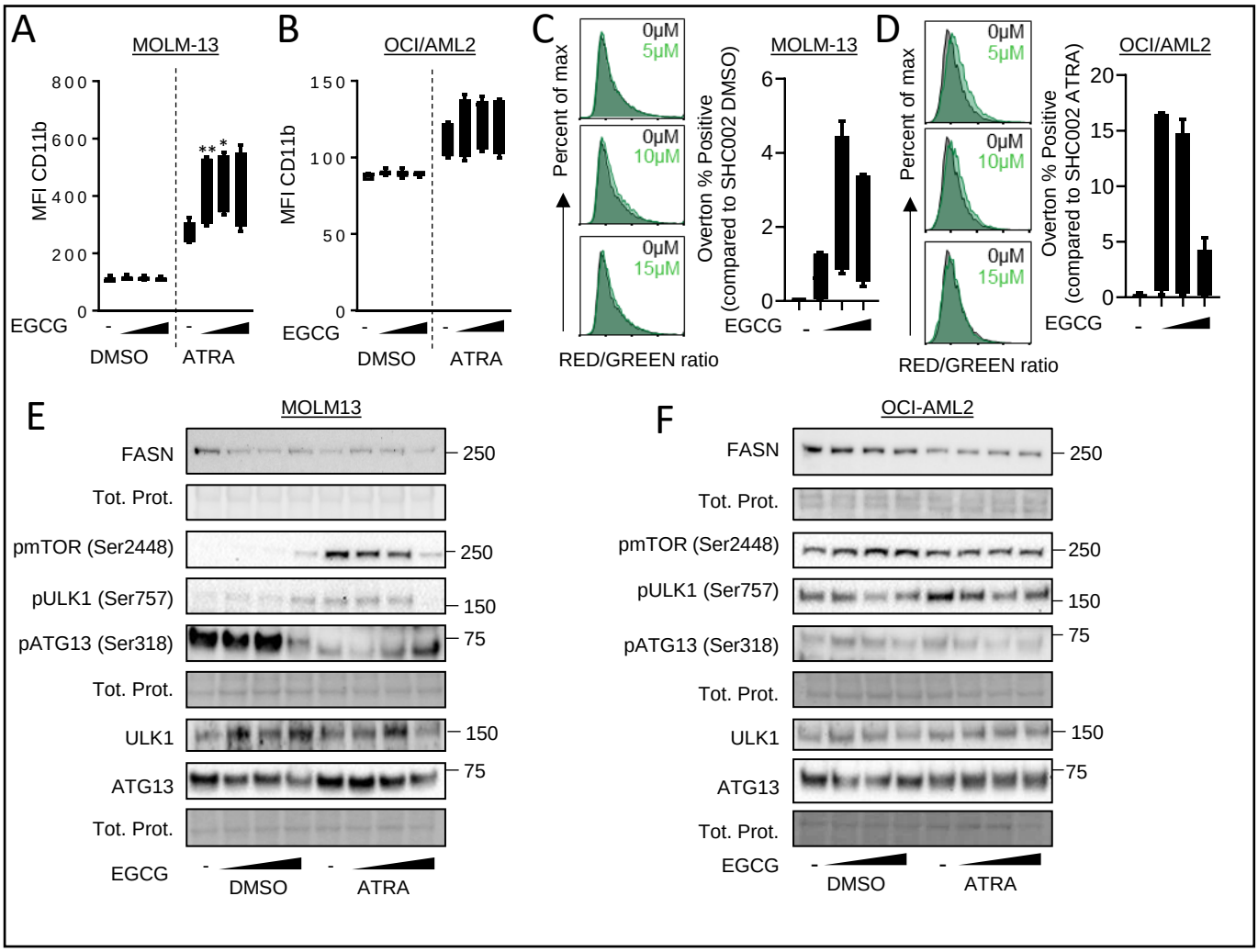
A
MOLM-13
MFI CD11b
800
600
400
200
0
**
*
EGCG
-
-
DMSO
ATRA
B
OCI/AML2
MFI CD11b
150
100
50
0
EGCG
-
-
DMSO
ATRA
C
Percent of max
0μM
5μM
0μM
10μM
0μM
15μM
RED/GREEN ratio
Overton % Positive
(compared to SHC002 DMSO)
MOLM-13
6
4
2
0
EGCG
-
D
Percent of max
0μM
5μM
0μM
10μM
0μM
15μM
RED/GREEN ratio
Overton % Positive
(compared to SHC002 ATRA)
OCI/AML2
20
15
10
5
0
EGCG
-
E
MOLM13
FASN
250
Tot. Prot.
pmTOR (Ser2448)
250
pULK1 (Ser757)
150
pATG13 (Ser318)
75
Tot. Prot.
ULK1
150
ATG13
75
Tot. Prot.
EGCG
-
-
DMSO
ATRA
F
OCI-AML2
FASN
250
Tot. Prot.
pmTOR (Ser2448)
250
pULK1 (Ser757)
150
pATG13 (Ser318)
75
Tot. Prot.
ULK1
150
ATG13
75
Tot. Prot.
EGCG
-
-
DMSO
ATRA

Figure 8

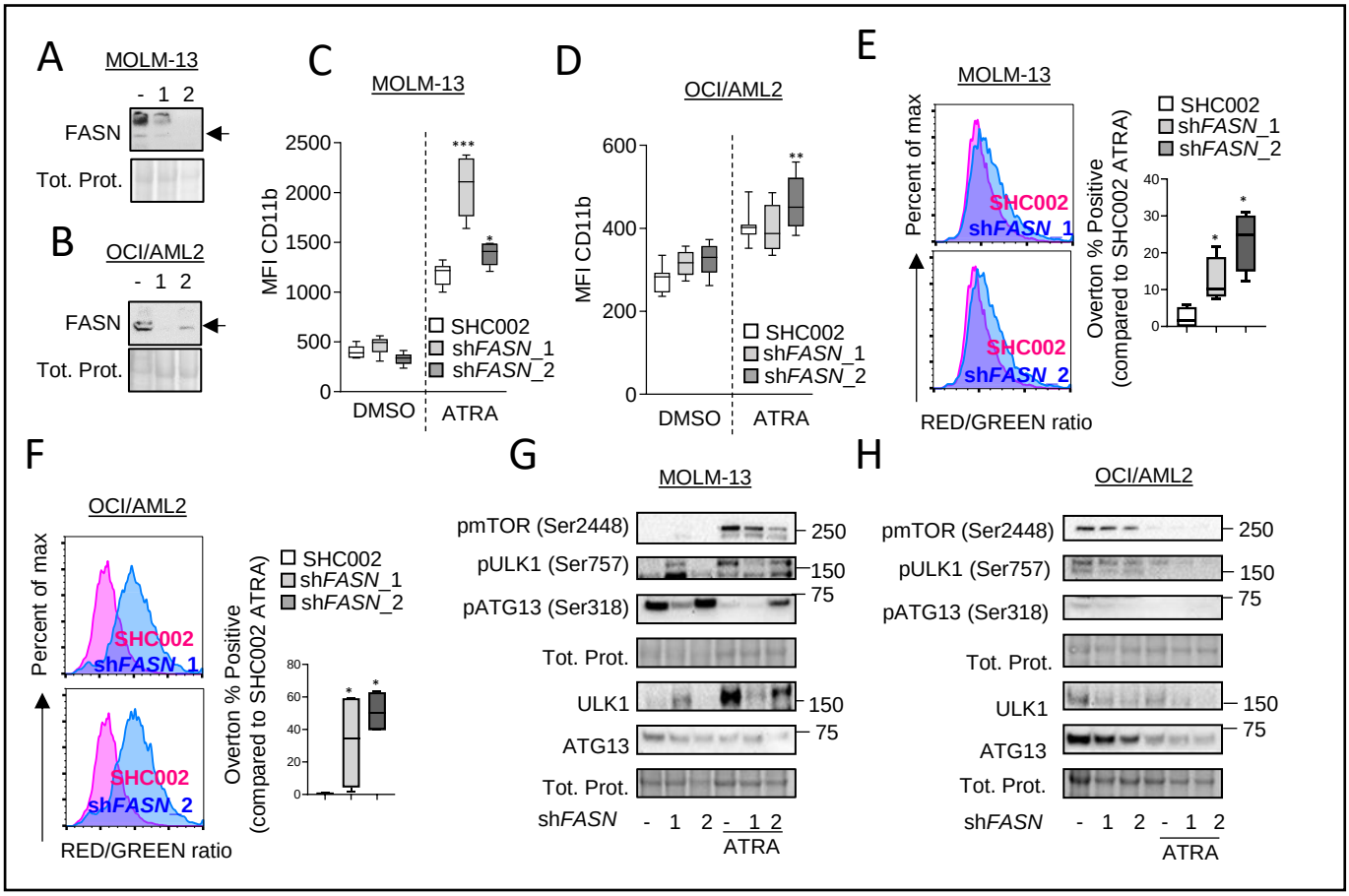
A
MOLM-13
- 1 2
FASN
Tot. Prot.
B
OCI/AML2
- 1 2
FASN
Tot. Prot.
C
MOLM-13
MFI CD11b
2500
2000
1500
1000
500
0
***
*
SHC002
shFASN_1
shFASN_2
DMSO
ATRA
D
OCI/AML2
MFI CD11b
600
400
200
0
**
SHC002
shFASN_1
shFASN_2
DMSO
ATRA
E
MOLM-13
Percent of max
SHC002
shFASN_1
SHC002
shFASN_2
RED/GREEN ratio
Overton % Positive
(compared to SHC002 ATRA)
40
30
20
10
0
*
*
SHC002
shFASN_1
shFASN_2
F
OCI/AML2
Percent of max
SHC002
shFASN_1
SHC002
shFASN_2
RED/GREEN ratio
Overton % Positive
(compared to SHC002 ATRA)
80
60
40
20
0
*
*
SHC002
shFASN_1
shFASN_2
G
MOLM-13
pmTOR (Ser2448)
pULK1 (Ser757)
pATG13 (Ser318)
Tot. Prot.
ULK1
ATG13
Tot. Prot.
250
150
75
150
75
shFASN - 1 2 - 1 2
ATRA
H
OCI/AML2
pmTOR (Ser2448)
pULK1 (Ser757)
pATG13 (Ser318)
Tot. Prot.
ULK1
ATG13
Tot. Prot.
250
150
75
150
75
shFASN - 1 2 - 1 2
ATRA